
DEVELOPMENT OF ANTIMICROBIAL PEPTIDES MIXTURES WITH ANTIBACTERIAL AND ANTI-INFLAMMATORY ACTIVITY

Angela Avitabile

Dottorato in Scienze Biotechologiche 29° ciclo
Indirizzo Biotecnologie Industriali e Molecolari
Università di Napoli Federico II



Dottorato in Scienze Biotecnologiche 29° ciclo
Indirizzo Biotecnologie Industriali e Molecolari
Università di Napoli Federico II



**DEVELOPMENT OF ANTIMICROBIAL
PEPTIDES MIXTURES WITH
ANTIBACTERIAL AND
ANTI-INFLAMMATORY ACTIVITY**

Angela Avitabile

Dottoranda: Angela Avitabile

Relatore: Prof. Alberto Di Donato

Coordinatore: Prof. Giovanni Sannia

A chi ha creduto in me.

INDEX

ABSTRACT	pag. 1
RIASSUNTO	pag. 2
Chapter 1-INTRODUCTION	
1.1 Antimicrobial peptides	pag. 7
1.2 Cryptic AMPs and AMP-releasing proteins	pag. 11
1.3 Additional biological activities of AMPs	pag. 11
1.4 Biotechnological application of AMPs	pag. 13
1.5 Pharmacological potential of AMP mixtures	pag. 13
1.6 Strategies for production of AMPs and AMP mixtures	pag. 14
1.7 Aims	pag. 18
Chapter 2-MATERIALS AND METHODS	
2.1 Materials	pag. 19
2.2 General procedures	pag. 19
2.3 Synthetic coding sequences	pag. 19
2.4 Bacterial growth culture media	pag. 19
2.5 Antibiotics	pag. 20
2.6 Expression of recombinant proteins	pag. 20
2.7 Purification of fusion proteins	pag. 20
2.8 Acid cleavage of Asp-Pro peptide bond	pag. 20
2.9 Purification of recombinant peptides	pag. 21
2.10 RP-HPLC	pag. 21
2.11 Antibacterial and antibiofilm assay	pag. 21
2.12 Bacterial strains used for antimicrobial susceptibility test	pag. 22
2.13 Mass spectrometry	pag. 22
Chapter 3-RESULTS AND DISCUSSION	
3.1 Production of CAMPS derived from the activation peptide of human pepsinogen	pag. 26
3.2 Antimicrobial activity	pag. 35
3.3 Antibiofilm assays	pag. 36
3.4 Designing of a carrier-less modular artificial precursor	pag. 41
3.5 Expression and purification of AT5H	pag. 44
3.6 Designing of a second carrier-less modular artificial precursor	pag. 47

3.7 Expression and purification of AT4LH	pag. 48
3.8 Cloning, expression and purification of ONC-AT2H	pag. 50
3.9 Antimicrobial activity of AT2H	pag. 53
Chapter 4-CONCLUSIONS	pag. 55
Chapter 5-PERIOD ABROAD	
5.1 Myxococcus xanthus	pag. 57
5.2 Frz system	pag. 59
5.3 Construction of a $\Delta frzA \Delta frzB frzB^{A\beta 4\beta 5}$ strain producing $FrzB^{A\beta 4\beta 5}$ Chimera	pag. 61
5.4 Production of a of $FrzCD \Delta 131-180$ mutant	pag. 64
5.5 Materials and methods	pag. 67
REFERENCES	pag. 68
APPENDICES	pag. 75

ABSTRACT

Antimicrobial peptides (AMPs) are relatively short peptides endowed with broad spectrum antimicrobial, anti-inflammatory immunomodulating and wound healing enhancement activity. They are essential components of the innate immune system of higher eukaryotes providing the first line of defense against microbial invasions. AMPs are extremely heterogeneous in length, structure, amino acid composition and, more importantly, molecular mechanism of bacterial killing. From this point of view AMPs can be divided in at least four wide classes: (i) cationic antimicrobial peptides (CAMPs); (ii) anionic antimicrobial peptides (AAMPs); (iii) histidine-rich antimicrobial peptides (HAMPs), and (iv) AMPs with intracellular targets (DNA, RNA, ribosomes, chaperons, enzymes).

The pharmacological potential of AMPs, and especially of AMP mixtures, is obvious. However the costs of pharmaceutical formulations including two or more peptides separately produced would be so high that even a very interesting pharmacological activity would not compensate for the effort needed to prepare the mixture. Accordingly, the aim of the present project is to develop a strategy to prepare mixtures of two or more AMPs with costs, production times and amount of work comparable to those necessary for the production of a single recombinant AMP.

Two alternative strategies were evaluated, one exploiting a previously optimized-carrier protein for the production of recombinant AMPs as fusion proteins, and an alternative strategy aiming to prepare a carrier-less precursor composed only by AMP modules.

The carrier developed by our group, ONC-DCless-H6, was able to effectively drive to inclusion bodies both a highly cationic sequence of about 50 residues [(P)PAP-A3(Pro26)] containing two CAMP-like sequences and a modular sequence (AT2H) of more than 100 residues including 2 anionic, 2 cationic and a histidine rich module. In both cases expression yields were high (>200 mg/L and >100 mg/L, respectively). Purification by IMAC provided a protein with good yield and purity. Purified recombinant proteins were hydrolyzed in 0.1 M acetic acid at 60°C to cleave the acid labile Asp-Pro sequences at the junction sites between consecutive AMP modules. The efficiency was very high in the case AT2H, which provided only the desired peptides, thus indicating that all the acid labile Asp-Pro sequences underwent cleavage with an efficiency higher than 95%. Only in the case of (P)PAP-A3(Pro26), the internal Asp-Pro sequence was cleaved with an efficiency of only about 85%. The comparison of the sequences adjacent to the different Asp-Pro cleavage sites in (P)PAP-A3(Pro26) and AT2H suggested that in order to obtain a very high cleavage efficiency a flexible sequence, rich in small and/or coil-preferring amino acids should be present at least on one side of the Asp-Pro site. This information will be useful for the design of further fusion proteins.

The carrier-less strategy was tested by preparing two modular precursors, AT5H (containing 5 anionic, 5 cationic and a histidine rich module) and AT4LH (containing 4 anionic, 4 cationic and a histidine rich module). AT5H and AT4LH showed relatively low expression levels (15 and 30 mg/L, respectively) and a different behavior of the inclusion bodies formed upon recombinant expression. In fact, the inclusion bodies, differently from those generated by ONC-DCless-H6, were soluble in 2 M urea thus suggesting a lower compactness/stability. A possible cause of the low expression levels could be the non-optimal codon usage of the coding sequences necessary for avoiding the presence of identical direct repeats which would have made difficult the chemical synthesis of the coding sequences. Low expression levels, in turn, could have contributed to the formation of "unstable" inclusion bodies. Indeed, it is well known that inclusion bodies formation is generally related to high expression levels. In the future, alternative approaches based on ligation of multiple copies of a smaller fragment could allow preparing coding sequences where all the repeats have an optimal codon usage.

RIASSUNTO

I Peptidi AntiMicrobici (AMP), sono peptidi relativamente corti dotati di attività antimicrobica ad ampio spettro. Sono componenti essenziali del sistema immunitario innato degli eucarioti superiori e rappresentano la prima linea di difesa contro le invasioni microbiche. Gli AMP sono estremamente eterogenei in lunghezza (da circa 15 a 50-60 residui), struttura secondaria e terziaria, composizione amminoacidica e meccanismo d'azione. Gli AMP possono essere divisi in almeno quattro classi:

- peptidi antimicrobici cationici (CAMP), il cui bersaglio sono le membrane;
- peptidi antimicrobici anionici (AAMP), il cui bersaglio sono i cationi metallici (e in secondo luogo le membrane);
- peptidi antimicrobici ricchi di istidine (HAMP), il cui bersaglio sono i cationi metallici (e in secondo luogo le membrane);
- AMP con bersagli intracellulari (DNA, RNA, ribosomi, enzimi).

Va ricordato che le 4 classi non sono ben separate. In particolare, molti AMP appartenenti alle prime tre classi possono possedere anche un bersaglio intracellulare. I CAMP hanno una carica netta positiva per l'abbondanza di residui di lisina e arginina e sono ricchi di residui idrofobici. Essi sono quindi in grado di acquisire una struttura anfipatica che permette loro di perturbare le membrane delle cellule batteriche e causarne la morte. Inoltre, alcuni CAMP interagiscono con bersagli intracellulari. Per esempio la Buforina II attraversa le membrane batteriche e si lega al DNA interferendo con la divisione cellulare e con la sintesi proteica.

AAMP e HAMP sono meno caratterizzati dei CAMP. In alcuni casi è stato dimostrato che la loro azione antimicrobica è dipendente dalla presenza di ioni metallici come, ad esempio, lo zinco: il complesso peptide/metallo si lega alle membrane batteriche compromettendone il funzionamento. Pertanto, sotto forma di complessi con i metalli, questi peptidi potrebbero mimare l'azione dei CAMP. Esempi sono la dermcidina, un AAMP presente nella pelle, e la "glicoproteina ricca di istidine", una delle più abbondanti proteine sieriche, caratterizzata dalla presenza di un dominio costituito da ripetizioni HXHXH.

Il peculiare meccanismo d'azione dei CAMP ne fa un'alternativa agli antibiotici convenzionali. Infatti, le cellule microbiche possono acquisire resistenza ai CAMP solo attraverso modifiche della loro composizione di membrana. Ma tale cambiamento non solo richiederebbe diverse mutazioni, ma potrebbe anche essere dannoso per lo stesso batterio poiché la membrana citoplasmatica possiede funzioni metaboliche essenziali tra cui la catena di trasporto degli elettroni e la sintesi di ATP. Le diverse classi di AMP verosimilmente cooperano tra loro così da ottimizzare l'azione battericida: AAMP e HAMP possono rallentare la crescita batterica sottraendo cationi metallici essenziali alla crescita; CAMP, AAMP e HAMP, possono uccidere direttamente i batteri, ma anche facilitare la penetrazione degli AMP che legano bersagli intracellulari. Ad esempio i CAMP capaci di legare gli LPS possono apportare danni alla membrana esterna aumentandone la permeabilità. Non sorprende quindi che tutti i fluidi corporei contengono miscele complesse di diversi AMP.

Il potenziale farmacologico degli AMP, e in particolare delle miscele di AMP, è evidente. Tuttavia, l'uso di peptidi come farmaci è ostacolata dagli elevati costi di produzione. Un peptide (o proteina) è preso in considerazione per lo sviluppo di un farmaco solo quando un farmaco convenzionale non è disponibile o il peptide è significativamente migliore rispetto al farmaco convenzionale dal punto di vista farmacologico. D'altra parte, i costi di una formulazione farmaceutica che includa due o più peptidi prodotti separatamente sarebbe così elevato che anche un'attività farmacologica molto interessante non compenserebbe lo sforzo necessario per preparare la miscela. Solo nel caso di una miscela di peptidi preparata dalla scissione

di una singola proteina precursore, i costi potrebbero essere sufficientemente contenuti da ipotizzarne una produzione a livello industriale.

Nel laboratorio dove si è svolto questo progetto di dottorato è stato sviluppato un sistema efficiente per la produzione di CAMP ricombinanti. Questi sono espressi fusi al C-terminale di un "carrier" derivato dell'onconasi (ONC-DCless-H6) una ribonucleasi che può essere espressa a livelli molto elevati all'interno di corpi inclusi (circa 150- 200 mg/L). Usando questa strategia diversi CAMP di lunghezza compresa tra 18 e 50 residui sono stati preparati ad una purezza maggiore del 98% con rese di circa 10-20 mg/L di cultura. Anche se efficiente questo metodo potrebbe essere ulteriormente ottimizzato. Ad esempio, un AMP di 20 residui viene prodotto a partire da un precursore di circa 130 residui. Così dopo la scissione del peptide desiderato 110 residui saranno scartati. Rese più elevate potrebbero essere ottenute aggiungendo più copie dell'AMP così da aumentare il rapporto AMP/ONC. Inoltre aggiungendo al carrier AMP differenti si potrebbe produrre una miscela di 2 o più AMP con la stessa procedura utilizzata per la produzione di un singolo AMP.

Infine, dati di letteratura suggeriscono che si possano produrre miscele di AMP con una strategia non basata su un carrier. Ad esempio la buforina II, un CAMP che lega il DNA, è stata prodotta sotto forma di concatenati (MMIS-M-buforin II-M-)_n dove MMIS è una sequenza anionica con densità di carica simile a quella della buforina che si è dimostrata essenziale per ottenere elevati livelli di espressione.

L'obiettivo generale di questo lavoro di ricerca è lo sviluppo di metodi efficaci per la produzione di miscele di due o più AMPs ricombinanti che possano essere preparate attraverso una singola linea di produzione rendendo così i costi comparabili a quelli di una singola proteina ricombinante.

Questo obiettivo è stato raggiunto attraverso due strategie:

I) Utilizzando il carrier ONC-DCless-H6 precedentemente sviluppato, secondo gli schemi:



dove "DP" è la sequenza acido-labile Asp-Pro necessaria per separare i moduli tra di loro e dal carrier.

II) Preparando precursori artificiali modulari privi di carrier contenenti moduli AAMP e CAMP alternati che possano essere idrolizzati in una miscela AMP secondo lo schema:



dove "TAG" è una breve sequenza tag o un AMP che può essere utilizzato come una sequenza tag durante la procedura di purificazione.

Produzione di CAMP derivati dal peptide di attivazione del Pepsinogeno

Al fine di verificare la possibilità di preparare proteine di fusione recanti più di un modulo CAMP, il peptide di attivazione della isoforma A3 del pepsinogeno (PAP-A3; 47 aa) è stato selezionato come CAMP modello. Uno strumento bioinformatico che permette l'identificazione di peptidi antimicrobici criptici all'interno di una sequenza proteica sviluppato dal nostro gruppo di ricerca suggeriva la presenza di due ipotetici CAMP corrispondenti ai primi 25 e agli ultimi 22 residui del peptide. Pertanto, PAP-A3 può essere considerato un esempio naturale di CAMP presenti in tandem in un precursore. Va notato che PAP-A3 contiene già un residuo di aspartato esattamente al limite previsto tra i due moduli (D25-F26). Pertanto, semplicemente inserendo un residuo di prolina tra i residui D25 e F26 è possibile ottenere un precursore contenente un sito sensibile all'idrolisi acida situato al confine tra i due moduli CAMP. Sono state quindi preparate due proteine di fusione ricombinanti, ONC-DCless-H6-(P) PAP-A3 e

ONC-DCless-H6-(P)PAP-A3(Pro26) che si differenziano per la presenza di una prolina. Le proteine sono state espresse in *E. coli* BL21(DE3) come corpi di inclusione a livelli molto elevati (circa 200-250 mg/L) e purificate mediante IMAC. La separazione dei CAMP dal carrier è stata ottenuta mediante idrolisi acida delle sequenze DP (in acido acetico/HCl pH 2). L'analisi SDS-PAGE ha mostrato che dopo 24 h di incubazione a 60°C, la sequenza DP che si trova nella regione linker di entrambe le proteine di fusione, è scissa efficientemente (circa il 95%). I peptidi sono stati purificati mediante precipitazione selettiva del carrier a pH 7,2.

Le due miscele di idrolisi sono state analizzate mediante RP-HPLC e spettrometria di massa che ha consentito di identificare tutti i frammenti attesi. Nel caso di ONC-DCless-H6-(P)PAP-A3 il 95% circa della miscela corrisponde al peptide desiderato (P)PAP-A3 e circa il 5% ai frammenti (P)IMY25 e FLK22 derivanti dall'idrolisi del legame Asp25-Phe26. Queste percentuali sono in accordo con le frequenze di idrolisi precedentemente determinate per sequenze Asp-X e dimostrano che il peptide desiderato di 47 residui può essere ottenuto con una perdita minima dovuta alla frammentazione del legame Asp25-Phe26. Nel caso di ONC-DCless-H6-(P)PAP-A3(Pro26) sono stati identificati i tre peptidi previsti (P)PAP-A3(Pro26), (P)IMY25 e (P)FLK22. Tuttavia, l'analisi quantitativa ha mostrato che solo l'80% circa del peptide è stato idrolizzato in corrispondenza del legame Asp25-Pro26. L'efficienza di idrolisi inferiore del sito Asp25-Pro26 rispetto alla sequenza Asp-Pro nella regione linker è probabilmente dovuta ad un maggiore ingombro sterico delle sequenze circostanti non presente nel linker tra carrier e peptide.

I peptidi sono stati purificati mediante RP-HPLC con un recupero di circa il 70%. La purezza dei peptidi è risultata essere superiore al 95%. (P)PAP-A3 è stato prodotto con una resa finale di circa 18-20 mg/L di coltura, mentre (P)IMY25 e (P)FLK22 sono stati prodotti con una resa finale di 7-8 mg/L della coltura per ciascun peptide. Pertanto, nonostante l'idrolisi incompleta del legame Asp25-Pro26, la strategia si è dimostrata adatta alla produzione contemporanea dei due peptidi ricombinanti.

Nei saggi di attività antimicrobica (P)PAP-A3 ha mostrato valori di MIC simili o addirittura inferiori a quelle del peptide di controllo GKY20 su un pannello ampio di ceppi Gram (-) e (+). Per quanto riguarda i frammenti, (P)IMY25 ha mostrato un'attività significativa su tutti i ceppi mentre (P)FLK22 è risultato attivo solo su due ceppi. Nei saggi di attività anti-biofilm invece i peptidi (P)IMY25 e (P)FLK22 si sono mostrati più attivi di PAP-A3. **Progettazione di precursori modulari privi di carrier**

Il secondo obiettivo di questo progetto di dottorato è stato la progettazione di un precursore modulare contenente moduli AAMP e CAMP alternati che formi corpi di inclusione non dannosi per l'ospite. Sono state progettate e sintetizzate due di tali proteine modulari:

MKQDP-(FibA-DP-GKY20-DP)₅-HRP (**AT5H**)

MKQDP-(FibA-DP-GKY20-DP)₂-L-(FibA-DP-GKY20-DP)₂-HRP (**AT4LH**)

Dove GKY20 è un CAMP derivato dal C-terminale della trombina umana (20 aa; carica = +5); FibA è il fibrinopeptide A, un AAMP (16 aa; carica = -3); HRP è un HAMP derivante dalla Histidine-rich glycoprotein umana (22 aa; carica = 0); L è un linker flessibile (6 aa; carica = 0). Le sequenze codificanti sono state ottenute mediante sintesi chimica. Solitamente durante la progettazione di una sequenza codificante sintetica, il codon usage viene adattato a quello dell'organismo ospite per ottenere elevati livelli di espressione. Tuttavia, nel caso delle sequenze codificanti AT5H e AT4LH questa strategia avrebbe comportato la presenza di 5 e 4 ripetizioni identiche, rispettivamente. Queste ripetizioni non solo rendono particolarmente difficile la preparazione del DNA sintetico ma potrebbero influenzare negativamente la

replicazione. Pertanto sono stati utilizzati due software, uno sviluppato da "GenScript" (AT5H) e uno da "Eurofin Genomics" (AT4LH) che permettono di minimizzare le ripetizioni sfruttando la degenerazione del codice genetico. Ovviamente questo ha reso impossibile rispettare pienamente il codon usage di *E. coli*.

Entrambe le proteine modulari AT5H e AT4LH hanno mostrato livelli di espressione relativamente bassi (15 e 30 mg/L, rispettivamente) e la formazione di corpi di inclusione, che, diversamente da quelli generati da ONC-DCless-H6, erano solubili in 2 M urea suggerendo una minore compattezza e/o stabilità. Una probabile causa dei bassi livelli di espressione potrebbe essere il codon usage non ottimale utilizzato per evitare la presenza delle ripetizioni nelle sequenze codificanti. I livelli di espressione bassi, a loro volta, potrebbero aver contribuito alla formazione di corpi di inclusione "instabili". Infatti, è noto che la formazione corpi di inclusione è associata generalmente ad elevati livelli di espressione.

Clonaggio, espressione e purificazione di ONC-AT2H

Dati i livelli di espressione insoddisfacenti di AT5H e AT4LH si è deciso di costruire una proteina di fusione, **ONC-AT2H**, unendo ONC-DCless-H6 con la metà C-terminale della proteina modulare AT4LH:



L'idrolisi acida completa di ONC-AT2H dovrebbe fornire una miscela di quattro peptidi nei seguenti rapporti molari: ONC-DCless-H6: (P) HRP: (P)FIBA(D): (P)GKY21 = 1: 1: 2: 2.

ONC- AT2H è stata espressa in *E. coli* BL21DE3 con una resa di circa 120 mg/L in forma di corpi inclusi resistenti al lavaggio con urea 2 M.

Mediante IMAC la proteina è stata purificata con una resa del 95% e una purezza superiore al 90%. ONC-AT2H è stata quindi idrolizzata a 60°C, pH 2 per 24 h e il carrier rimosso mediante precipitazione frazionata. Mediante RP-HPLC e spettrometria di massa si è accertato che la miscela conteneva essenzialmente solo i tre peptidi attesi. La resa è stata di circa 15-16 mg della miscela di peptidi per litro di coltura. Confrontando i risultati con quelli ottenuti nel caso delle due proteine modulari si può concludere che ONC-AT2H fornisce rese più elevate con una procedura di purificazione semplice.

Per studiare l'attività antimicrobica della miscela sono state effettuate curve dose-effetto utilizzando (P)GKY20 e (P)GKY21 purificato dalla miscela come controlli.

(P)GKY20 e (P)GKY21 hanno mostrato sostanzialmente la stessa attività mentre la miscela contenente anche (P)FIBA(D) e (P)HRP è risultata considerevolmente più attiva suggerendo che questi due AMP contribuiscono all'attività antimicrobica. Resta da determinare se l'attività della miscela sia la somma dei contributi dei tre peptidi o se invece non siano presenti interazioni di tipo sinergico.

In conclusione, è possibile affermare che, anche se non tutti gli obiettivi iniziali sono stati pienamente raggiunti, questo lavoro di dottorato potrà aprire la strada allo sviluppo di miscele di peptidi farmacologicamente interessanti.

Attività di ricerca svolta presso il laboratorio diretto dal Dott. Tam Mignot.

Durante il periodo di ricerca all'estero, della durata di tre mesi, sono stata ospite presso il CNRS di Marsiglia nel Laboratorio di Chimica Batteriologia (LCB) del Dott. Tam Mignot.

Il mio progetto ha previsto l'individuazione di punti di controllo nel sistema di regolazione chemiotattico di *Myxococcus xanthus*.

M. xanthus è un batterio del suolo che cresce comunemente in terreno umido ricco di sostanza organica e che si muove con due sistemi geneticamente distinti. Il primo

sistema è chiamato sociale, (S) motility, e comporta il movimento delle cellule all'interno del gruppo. Il secondo sistema è chiamato avventuroso, (A) motility, e comporta il movimento delle singole cellule. Le cellule di *M. xanthus* invertono periodicamente la loro direzione di movimento e si pensa che queste inversioni cellulari siano necessarie nella regolazione della chemiotassi. In natura, quando cellule di *M. xanthus* non sono in grado di trovare le sostanze nutrienti sufficienti, entrano in un processo di sviluppo in cui si aggregano formando cumuli pigmentati, chiamati corpi fruttiferi. All'interno dei corpi fruttiferi, le cellule si differenziano per formare spore che sono cellule metabolicamente dormienti resistenti a periodi prolungati di digiuno, essiccazione, e temperature relativamente elevate.

Il sistema chemiotattico Frz dirige la motilità in *M. xanthus* regolando la frequenza di reverzione cellulare. Il sistema Frz è composto da: FrzCD, un chemiorecettore citoplasmatico; FrzA e FrzB, due proteine CheW-like; FrzE, una proteina di fusione CheA-CheY; FrzF, una metiltransferasi; FrzG, una metilesterasi; e FrzZ, una fusione CheY-CheY. Partendo da queste premesse il progetto ha previsto:

i) La costruzione del ceppo $\Delta frzA \Delta frzB frzB^{A\beta 4\beta 5}$ per produrre la Chimera $FrzB^{A\beta 4\beta 5}$.

Il sistema Frz, presenta due proteine CheW-like, FrzA e FrzB. Ci siamo chiesti perché il sistema Frz avesse bisogno di due CheW-like. Da analisi cristallografiche è emerso che una regione di 20 amminoacidi che forma due foglietti beta, è presente in FrzA ma non in FrzB. Questo suggerisce che FrzB manca della regione di legame a FrzE.

Abbiamo quindi costruito un ceppo ricombinante produttore una proteina chimerica chiamata $FrzB^{A\beta 4\beta 5}$, ottenuta con l'introduzione dei 21 amminoacidi formanti i due foglietti beta di FrzA, in FrzB. Il ceppo risultante, $\Delta frzA \Delta frzB frzB^{A\beta 4\beta 5}$, ha risposto all'IAA (isoammil alcool, un attivatore del sistema), il che significa che la chimera può legarsi all'istidin-chinasi e FrzA è la CheW-like principale del sistema.

ii) Produzione del mutante $FrzCD\Delta 131-180$.

I recettori canonici di *E. coli*, comprendono un dominio transmembrana, un dominio di legame al ligando, un dominio HAMP, ed una regione di segnalazione. L'HAMP è una regione flessibile che cambia quando i recettori rilevano il segnale e trasferiscono il cambiamento conformazionale al dominio di metilazione. Invece, il recettore FrzCD di *M. xanthus*, non ha domini transmembrana ed ha un dominio HAMP degenerato. E' quindi un recettore citoplasmatico. La regione che si estende dall'amminoacido 7 al 27 ha amminoacidi carichi positivamente, ed ha un ruolo molto importante nel legame al DNA, mentre la regione che va da 131 a 180 ha una funzione ancora sconosciuta.

Per comprendere il ruolo della porzione 131-180 ho effettuato la delezione di questa stessa, ed ho quindi creato il mutante chiamato $frzCD\Delta 131-180$.

Dopo aver ottenuto il plasmide ho richiesto il suo sequenziamento. Ho utilizzato questo plasmide per trasformare *M. xanthus* e attraverso il metodo della doppia selezione e ricombinazione ho ottenuto il mutante. Una volta effettuato uno screening delle colonie, ho effettuato la selezione con il galattosio. Avendo utilizzato un sistema di doppio ricombinante, questo tipo di selezione mi ha garantito che le colonie che presentavano un alone hanno subito una singola ricombinazione, rappresentando quindi le WT, mentre quelle che non presentano un alone hanno subito la doppia ricombinazione e pertanto rappresentavano i mutanti di interesse.

Questo perché se avviene una singola ricombinazione, il gene wt verrà ricostituito, mentre se si verificano entrambe le ricombinazioni ci sarà un riarrangiamento dei geni e si otterrà il nostro mutante di interesse.

Nella nostra analisi del fenotipo, il mutante $frzCD\Delta 131-180$, non mostra né espansione delle colonie né corpi fruttiferi. Questo fenotipo è dovuto al fatto che le cellule sono in iper-reversione e non possono produrre un affollamento netto.

Chapter 1-Introduction

1.1 Antimicrobial peptides

Antimicrobial peptides (AMPs) are relatively short peptides endowed with a broad spectrum of antimicrobial activity (Fig. 1.1). They are essential components of the innate immune system of higher eukaryotes providing the first line of defense against microbial invasions. AMPs are extremely heterogeneous in length (from about 15 to 50-60 residues), secondary/tertiary structure (Fig. 1.2), amino acid composition and, more importantly, molecular mechanism of bacterial killing. From this point of view AMPs can be divided in at least four classes:

- I. cationic antimicrobial peptides (CAMPs) which target membranes.
- II. anionic antimicrobial peptides (AAMPs) which target metal cations (and membranes).
- III. Histidine-rich antimicrobial peptides (HAMPs) which target metal cations (and membranes).
- IV. AMPs with intracellular targets (DNA, RNA, ribosomes, chaperons, enzymes).

However, it should be remembered that the 4 classes are not well separated. In particular, several AMPs belonging to the first three classes sometimes also interact with intracellular targets.

CAMPs, as their name suggests, have a positive net charge due to the abundance in lysine and arginine residues and are rich in hydrophobic residues. They are consequently able to acquire an amphipathic structure which allows them to perturb bacterial membranes, their main target, leading to cell death (Fig. 1.3). The net positive charge drives the initial adsorption to the surface of bacterial membranes, very rich in negative charges due to anionic lipids such as phosphatidylglycerol or lipopolysaccharides. The amphipathic nature of CAMPs causes their insertion into the membrane and the opening of pores which cause osmotic lysis [1]. On the contrary, in eukaryotic membranes, anionic phospholipids are sequestered in the inner leaflet and thus no electrostatic interaction can be established [2]. This important molecular feature is the basis of the selectivity of CAMPs towards bacteria. It should be reminded however, as already mentioned, that some CAMPs have intracellular targets. For example, Buforin II crosses bacterial membranes and binds to DNA, interfering with cell division and protein synthesis.

AAMP and HAMPs are less known than CAMPs. In some cases, it has been demonstrated that the antimicrobial action of these AMPs is dependent on the presence of metal ions like zinc: the metal/peptide complex would bind to the bacterial membranes thus impairing their function. Therefore, in the metal bound form, these peptides would mimic CAMPs. Examples are dermcidin, an AAMP present in the skin, and Histidin-rich glycoprotein, a HAMP of serum, and three small antimicrobial anionic peptides (SAAPs), GA(D)₅, G(D)₆, and (D)₇, present in pulmonary surfactant. SAAPs are peculiar as they also interact with an intracellular target. In the presence of zinc, they penetrate membranes without inducing any morphological change. Once in the cytoplasm, SAAPs bind to and inhibit ribosomes.

However, it has been suggested that AAMPs and HAMPs could also exert an indirect antimicrobial effect by scavenging essential metals (Zn, Fe, Cu, Mn, Co etc.), thus impairing bacterial growth.

In higher eukaryotes AMPs are secreted by many cell types in several different tissues. Moreover, some AMPs are expressed constitutively, whereas other are finely modulated. Very interestingly several AMPs are expressed constitutively at

low levels but their expression can be increased in response to different stimuli. The regulation of expression is particularly well known in the case of human CAMPs, the cathelicidin LL-37 and the alpha and beta defensins ([3] and references therein). For example, LL-37 is expressed constitutively in many cell types but in epithelial cell its expression is modulated by inflammatory triggers such as wounding or infections [3]. In addition, the expression of LL-37 is induced by vitamin D3. Human beta defensin 1 (HBD1) is constitutively expressed in epithelial cells, whereas human beta defensins 2 and 3 are induced by NF- κ B and TNF, respectively ([3] and references therein). Finally human beta defensin 4 is induced by the combined action of bacteria and TNF ([3] and references therein).

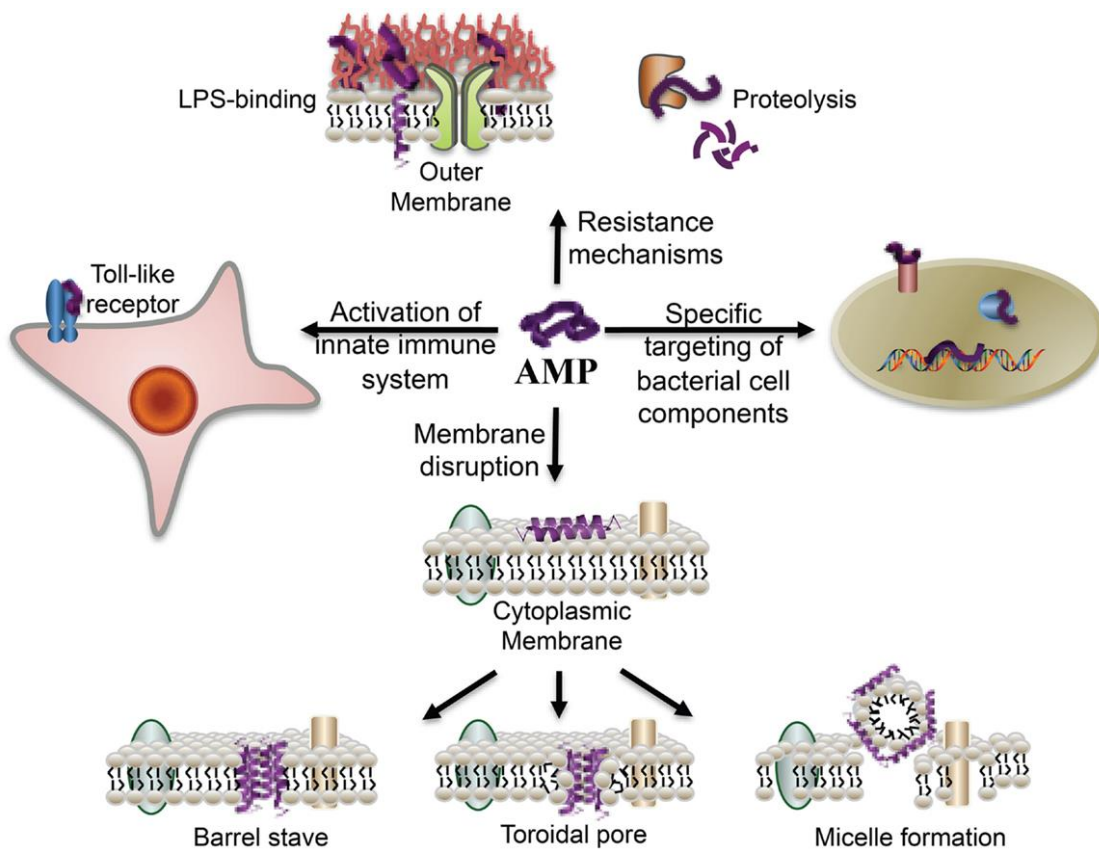


Figure 1.1: Schematic representation of multiple action of antimicrobial peptides. AMP, anti-microbial peptide; LPS, lipopolysaccharide.

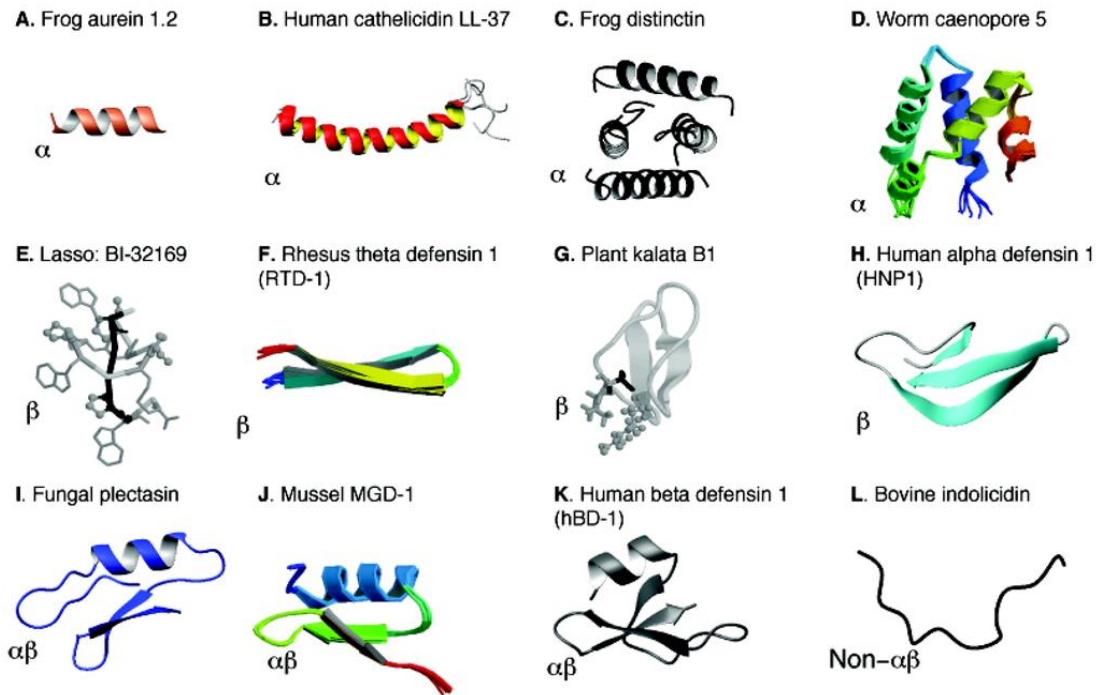


Figure 1.2: Example of structures of antimicrobial peptides.

Structural diversity and classification of natural antimicrobial peptides. The known structures of AMPs are classified into four families (α , β , $\alpha\beta$, and non- $\alpha\beta$) and the structural family for each peptide is indicated at the left bottom corner of each panel. (from Wang G. 2013)

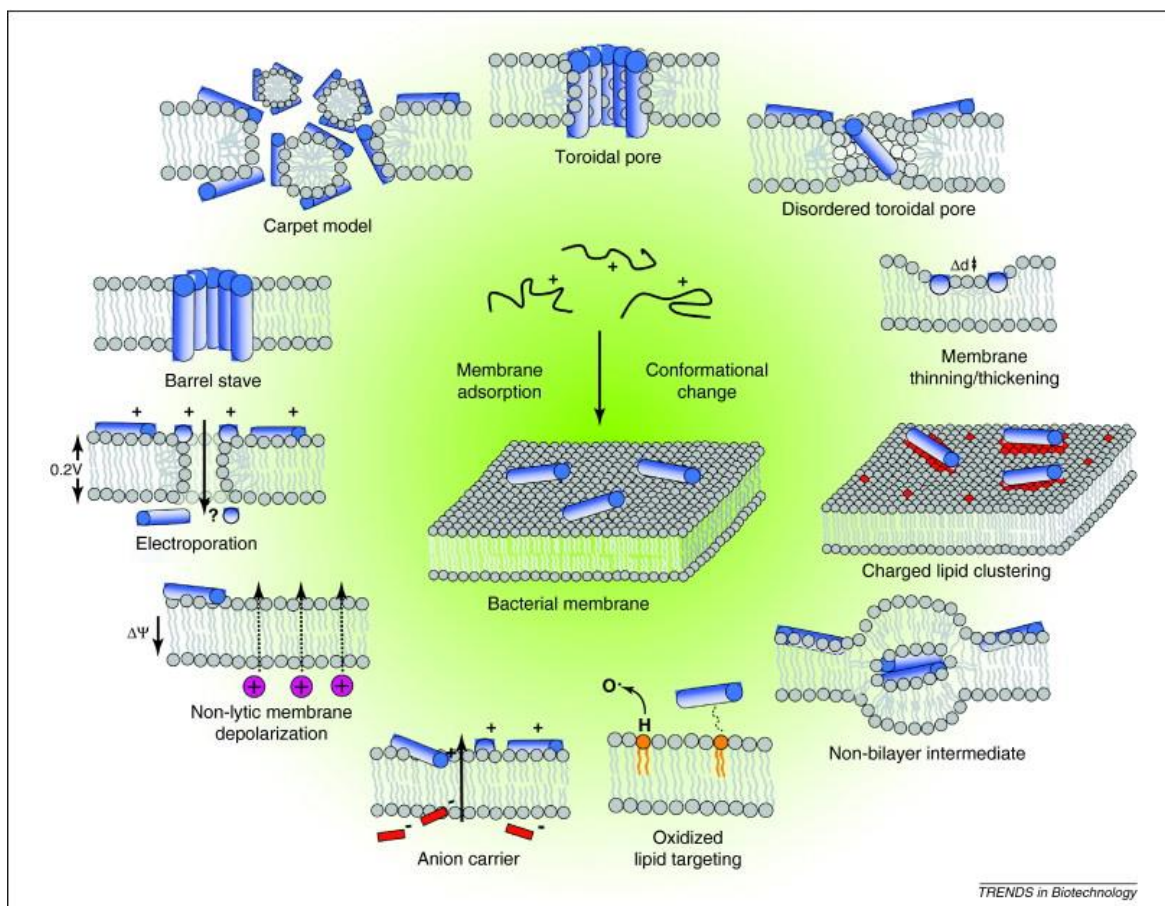


Figure 1.3: Key mechanisms of bacterial membrane disruption by antimicrobial peptides.

Events occurring at the bacterial cytoplasmic membrane following initial antimicrobial peptide (AMP) adsorption. These events are not necessarily exclusive of each other. In the classical models of membrane disruption, the peptides lying on the membrane reach a threshold concentration and insert across the membrane to form either peptide-lined pores in the barrel-stave model, solubilize the membrane into micellar structures in the carpet model, or form peptide-and-lipid-lined pores in the toroidal pore model. In the revised disordered toroidal pore model, pore formation is more stochastic and involves fewer peptides. The thickness of the bilayer can be affected by the presence of the peptides, or the membrane itself can be remodeled to form domains rich in anionic lipids surrounding the peptides. In more specific cases, non-bilayer intermediates in the membrane can be induced; peptide adsorption to the membrane can be enhanced by targeting them to oxidized phospholipids; a peptide may couple with small anions across the bilayer, resulting in their efflux; the membrane potential can be dissipated without other noticeable damage; or conversely, in the molecular electroporation model, the accumulation of peptide on the outer leaflet increases the membrane potential above a threshold that renders the membrane transiently permeable to various molecules including the peptides themselves. (from Leonard T. Nguyen, 2011).

1.2 Cryptic AMPs and AMP-releasing proteins

Microbial cells might acquire resistance to CAMPs and other membrane targeting AMPs only through the modification of the membrane composition [1]. Such a change not only would require several mutations, but could also be detrimental to bacterial cells as their cytoplasmic membrane has several essential metabolic functions including electron transport chains and ATP synthesis.

However, some strains have acquired a limited resistance to antimicrobial peptides by producing specific proteases like, for example, “omptins” of enterobacteria and V8 proteases of *Staphylococcus* ssp. [4-5]. However, multicellular eukaryotes have developed a very interesting countermove to defend from the attack of bacterial cells: the secretion of “AMP-Releasing Proteins” (AMP-RPs, usually >100 aa) which release active peptides only after a partial proteolytic processing operated by host and/or bacterial proteases. Thus, a bacterial strain that secretes proteases to escape AMPs would “suicide” by releasing “cryptic” AMPs from these precursors. This mechanism has been demonstrated for Zf-3 a ribonuclease from *Danio rerio* [6]. Surprisingly, several proteins with functions not necessarily related to host defense can behave as sources of CAMPs. Some examples are hemoglobin, thrombin, lactoferrin, lysozymes, histone-like proteins and vertebrate secretory ribonuclease. Lysozyme is a well-known example: it exerts bactericidal action by hydrolyzing peptidoglycan but, if inactivated by proteolysis, it releases CAMPs [7]. It is well established that mammalian’s lactoferrin, a multifunctional protein, possesses bactericidal determinants in the positively charged helix at the N-terminus. Proteolysis in the stomach of infants leads to the release of a 25-aa peptide, which is more bactericidal than the native protein on several strains, including antibiotic-resistant strains [8-9]. More recently it has been demonstrated that human thrombin, a key enzyme in the coagulation cascade, contains bactericidal determinants in the C-terminal region. It is worth noting that a peptide deriving from this region of thrombin has been detected *in vivo* in human wounds [10-11].

Also fibrinopeptides are examples of “cryptic” AAMPs. In fact, these small anionic peptides that are released from fibrinogen to allow the formation of the fibrin cloth, have also antimicrobial activity.

1.3 Additional biological activities of AMPs

In addition to direct bacteria killing some CAMPs have key modulatory functions in the innate immune response including the ability to inhibit LPS-induced production of proinflammatory cytokines, chemotaxis, induction of cytokine release and anti-inflammatory activity [12]. For example, some α and β defensins, CAMPs present in human skin, are chemotactic for T lymphocytes, monocytes and immature dendritic cells. *In vivo* studies showed that some CAMPs, like LL-37, stimulate macrophages to produce chemokines which in turn attract additional cells to the inflamed sites [13]. Several CAMPs protect the host against potentially lethal effects resulting from an excessive TLR-mediated inflammatory response induced by lipopolysaccharide (LPS) and other bacterial “endotoxin” by altering gene expression of various inflammatory cells [14]. The endotoxin-neutralizing activities is typical of many well-known CAMPs (LL-37, PR-39) [15] but is also found in recently identified CAMPs, like the thrombin-derived peptide which exerts immunomodulatory functions by inhibiting macrophage responses to bacterial lipopolysaccharide [10-16]. Thus, CAMPs can be considered as a bridge between innate and adaptive immunity.

Finally CAMPs promote wound healing [15]. Wound healing requires an orchestrated integration of complex cellular events involving hemostasis, inflammation, remodeling, angiogenesis, tissue formation and re-epithelialization [13]. Some CAMPs strongly expressed in skin epithelium during wound healing, like cathelicidins (e.g. LL-37), are involved in all phases of tissue repair including angiogenesis [13-17-18]. Interestingly, Ramos *et al.* demonstrated *in vivo* that antimicrobial peptide, LL-37, can be used topically to stimulate wound healing in a diabetic mice model [15].

Also some AAMPs show additional biological activities. For example, the structure of SAAPs present in pulmonary surfactant is similar to the charge-neutralizing pro-peptides of Group I serine proteases. In particular, it has been demonstrated that they are trypsin inhibitors [19]. Therefore, SAAPs can regulate the activity of pulmonary proteases.

These findings suggest that the potential pharmacological applications of AMPs are not limited to antibacterial therapy but include stimulation of immune system, tissue repair and wound healing.

1.4 Biotechnological application of AMPs

AMPs biotechnological applications span from pharmaceutical industry to food industry. They are gaining attention mainly as antimicrobial alternatives, food preservatives and recently as immune defense regulators. Some AMPs, are already in phase II/III clinical trial as antimicrobials restricted to topical applications [4-14].

For anti-infective purposes, the first AMPs to be commercially manufactured were gramicidins produced by *Bacillus brevis* [20] used as antibiotics for topical applications. Other examples are nisin, approved since 1969 [21], and lactoferrin added to infant milk formula [22], both used in food industry as natural preservatives or dietary supplements. Currently, application of antimicrobial peptides in the medical field is still one of the most interesting perspective. The ability of AMPs to modulate the innate immune system has made them promising candidates also as vaccine adjuvants [14]. The inclusion of appropriate adjuvants in vaccines helps to improve their efficacy. Evidences are based on several observations such as human neutrophil defensins that can enhance both humoral and cell-mediated antigen- specific immune response in murine models [23].

Moreover, using natural peptides as templates, synthetic peptides have been designed that retain the immunomodulatory properties but lack unwanted effects like mast cell degranulation exerted by certain natural AMPs as the bovine peptide bactenecin. The resulting molecules, named IDR peptides (Innate Defense Regulators) boost protective immunity against infections without possessing direct antimicrobial action [24]. Nowadays many IDR-peptides are in clinical trial for topical application. An example is IMX-492 that has recently completed phase I clinical trials in patients with cancer chemotherapy-induced immune suppression [4-14]. Other peptides, such as MX-226 and Hlf1-11, were originally developed as antimicrobial peptides but later showed interesting immunomodulatory activities [4]. Thus, there are ample opportunities to develop AMPs for clinic use as anti-infective agents.

1.5 Pharmacological potential of AMP mixtures

Different classes of AMPs can cooperate to optimize bacterial killing. Metal scavengers (AAMPs and HAMPs) can slow down bacterial growth by subtracting essential nutrients. Membrane damaging peptides (CAMPs, AAMPs and HAMPs) can directly kill bacteria but also facilitate the penetration of AMPs that bind intracellular targets. AAMPs with protease inhibition activity can extend the life of AMPs and exert anti-inflammatory activity. LPS-binding CAMPs can both directly damage the outer membrane and act as LPS scavengers with anti-inflammatory activity.

Not surprisingly all body fluids contain complex mixtures of different AMPs. Blood contains defensins, His-rich glycoprotein, several CAMPs and AAMPs derived from platelets and an undefined number of AMP-releasing proteins (e.g. thrombin, fibrinogen, apolipoproteins and, likely, many others). Skin constitutively produces dermcidin and psoriasin (two AAMPs) and in an inducible manner defensins and cathelicidins (CAMPs). The surfactant of airways contains both AAMPs and CAMPs.

The pharmacological potential of AMPs and especially of AMP mixtures is obvious. These peptides could be used to integrate and potentiate conventional antibiotics when these molecules are ineffective due to the development of multidrug resistant

strains or the formation of biofilm. At the same time, they would provide anti-inflammatory, wound healing and immunomodulatory activities.

However, the use of peptides as drugs is hampered by the high production costs. Usually a peptide (or a protein) is used as a drug only when a conventional drug is not available or the peptide is significantly better than the drug from the pharmacological point of view. On the other hand, the costs of a pharmaceutical formulation including two or more peptides separately produced would be so high that even a very interesting pharmacological activity would not compensate for the effort needed to prepare the mixture.

Only in the case of a peptide mixture prepared from the cleavage of a single precursor protein the costs could be adequate to hypothesize a scale up to the industrial level. Several results described in literature suggest that it is possible to project a “modular” artificial precursor protein whose cleavage would provide the desired mixture of biologically active peptides.

1.6 Strategies for production of AMPs and AMP mixtures

Chemical synthesis and biological production methods are the most popular techniques for production of peptides.

Chemical synthesis is particularly well suited when a relatively small amount of peptide is required and when the peptide is shorter than about 30 residues [25]. However, as the biotechnological application of these molecules cannot overlook production costs, biological production methods can be potentially more attractive for large scale production.

E. coli is a common microbial platform for AMPs production [26-27] due to its well-known biology, for the availability of cloning vectors and cheap media for cell growth.

The main concerns in developing an AMP production platform using bacterial expression systems are: (i) AMP toxicity for the host, ii) AMP intracellular degradation by proteases leading to low yields and iii) peptide purification.

These difficulties can be circumvented by fusing the desired peptides to a carrier protein that can protect peptides from proteases, neutralize possible toxic effects and provide a convenient system for their purification.

By now, more than 30 kinds of fusion tags with different sizes and functions have been used for AMPs expression. Some examples are: thioredoxin (Trx), glutathione S-transferase (GST), maltose binding protein (MBP), intein-mediated systems [28].

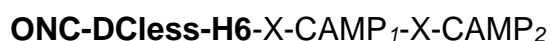
However, also fusion protein strategy has two main drawbacks. First, the fusion protein must be cleaved and the peptide needs to be separated from the carrier. Second, the desired peptide usually represents just a small percentage of the purified fusion protein. As for the cleavage of the peptide, it can be released from the fusion protein by enzymatic or chemical cleavage at a site suitably introduced at the carrier-peptide junction [27]. The efficiency and specificity of the cleavage is the main bottleneck of fused peptide production. Usually enzymatic proteolysis by factor Xa [29-30], enterokinase [31] and thrombin [32-33], the most used enzymes, is less efficient than chemical cleavage [34]. On the other hand, the most popular cleavage reagents, like cyanogen bromide (CNBr), formic acid and hydroxylamine, [34], often produce unwanted cleavages and side-chain modifications due to the harsh reaction conditions needed for the cleavage [34].

In the laboratory where this PhD project has been developed a method for the production of recombinant AMPs has already been optimized [35]. AMPs are

expressed as fusion proteins by attaching the desired peptide to the C-terminus of onconase (ONC) a frog ribonuclease from *Rana pipiens* [36]. ONC is a very well suited carrier for several reasons: (i) it can be expressed at very high levels in inclusion bodies (about 200-250 mg/L in Terrific Broth); (ii) usually, no soluble ONC can be detected in cultures thus minimizing the risk of toxic effects of the ONC-peptide fusion proteins; (iii) it is a very small protein (104 aa) thus allowing high yields of the peptides after the cleavage; (iv) the solubility of denatured onconase is pH dependent – the denatured protein is soluble only at pH <4 – thus allowing the purification of peptides soluble at pH 7 by selective precipitation of the carrier. Moreover, ONC does not contain Asp-Pro and Asn-Gly sequences and the mutant (M23L)-ONC [37] does not contain internal methionine residues, therefore onconase carrier will not be cleaved by all common chemical cleavage strategies such as formic acid, which cleaves the bond between aspartate and proline, cyanogen bromide, which cleaves Met-X bonds and hydroxylamine, which cleaves the bond between asparagine and glycine [38]. In order to improve its efficiency as a carrier (M23L)-ONC was further engineered by site directed mutagenesis. All the aspartate residues were changed to glutamate as, even if at very low frequency, all the Asp-X sequences undergo cleavage in acidic conditions. These cleavage events would cause the release of undesired ONC derived fragments thus making more complex the purification of the AMP. The eight cysteine residues in (M23L)-ONC were mutated to hydrophobic residues (leucine, isoleucine or tyrosine) to avoid the formation of undesired oxidation products during the purification. A His6 tag was added at the C-terminus of ONC thus allowing the purification of the fusion protein by metal chelate affinity chromatography. The final carrier has been named ONC-DCless-H6.

We tested the efficiency of our strategy by producing GKY20, a short cationic antimicrobial peptide derived from the C-terminus of human thrombin [16] active on different strains of *E. coli* with a minimal inhibitory concentration (MIC) lower than 10 µM. Peptide GKY20, was fused to ONC-DCless-H6 through a linker sequence ending with the acid cleavable aspartyl-prolyl sequence (Fig. 1.4). The recombinant peptide (P)GKY20 was purified according to the strategy shown in Figure 1.4 with a final purity of about 96% and a yield of about 15 mg per L of culture. The method has been already used to prepare three further cryptic CAMPs, from human apolipoproteins E and B, with lengths of 18, 25 and 37 residues [39-40]. All these peptides were obtained with yields higher than 10 mg/L of culture thus demonstrating the general applicability of the method.

Even if efficient this method could be further optimized. In fact, if a 20-residue long peptide is produced from a precursor of about 130 residues, after the cleavage 110 residues out of 130 are discharged. Higher yields could be obtained by appending to ONC more AMP “modules”, either identical or even different as in the schemes below:



where X is a suited cleavage sequence (e.g. Asp-Pro, Met, Asn-Gly etc.) and “n” the number of repeats. CAMP₁, CAMP₂ and CAMP₃ are different CAMPs which would

be obtained as a mixture after the cleavage of the precursor and selective precipitation of the carrier.

On the other hand, J. H. Lee and coworkers [41] conceived an alternative strategy not based on the use of a carrier protein to prepare buforin II, a cryptic CAMP deriving from histone H2A. Initially they prepared head to tail multimers of buforin alone (from 2 to 6 repeats). These multimers showed very low expression levels. Moreover, expression levels decreased by increasing the number of repeats. These results were attributed by the authors to the toxicity generated by the very high positive charge of the multimers, indeed each buforin module has a net charge = +7 so that the (buforin II)₆ multimer, 120 residues long, has a net charge = +42. Thus, an alternative strategy was used, based on the natural secretion system of another type of CAMP, magainins. These are frog CAMPs, present at high concentration in skin secretions. They are produced as large precursors containing several magainin copies separated by repeats of an acidic module called MIS (Magainin Intervening Sequences). After secretion, proteases cleave the precursor releasing the magainin modules [42]. Thus, Lee and coworkers designed a “modified MIS” (MMIS) and prepared a modular protein composed by alternating copies of MMIS and buforin II:



where $n = 2-6$ and M are methionine residues necessary to cleave the precursor by CNBr. It is worth to note that the MMIS modules had the same length and charge density of buforin. Thus each repeat MMIS-M-buforin II-M was globally neutral. Differently from buforin II multimers the new modular proteins were expressed at very high levels in inclusion bodies.

We decided to use a modified Lee’s strategy using as neutralization acidic peptide an AAMP i.e. a peptide endowed itself with a antimicrobial activity and able to contribute to the pharmacological activity of the mixture after the cleavage of the precursor.

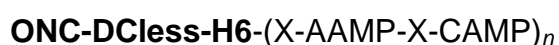
The general structure of such a precursor can be described by the scheme:



where X is a suited cleavage sequence and “n”, the number of repeats.

Once cleaved, these artificial fusion proteins would immediately provide a mixture of CAMPs and AAMPs whose pharmacological applications could be wider than those of the single AMPs.

In principle it could also be possible to design precursor containing two or more different CAMP modules and two or more different AAMP modules as well as to insert further functional peptides like for example histidine-rich or proline-rich AMPs. Moreover, if necessary, these modular precursors could also be attached at the C-terminus of carriers like ONC-DCless-H6 to increase expression levels:



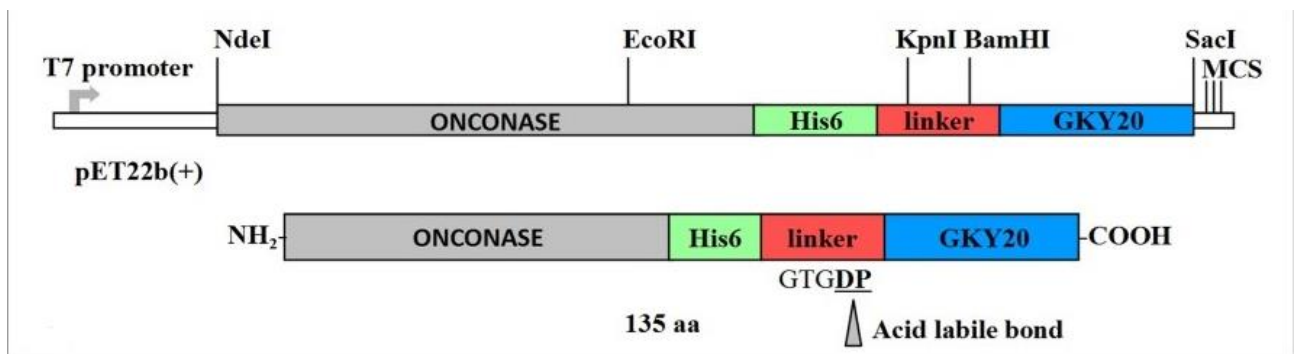


Figure 1.4: Schematic representation of expression vector and recombinant protein.
 (from Pane K. et al. 2016).

1.7 Aims

The general aim of this research work is the development of effective methods for the production of mixture of two or more recombinant AMPs with additive and/or synergistic activity that can be produced as a single precursor protein i.e. a mixture of AMPs that not only should be very interesting from the pharmacological point of view but that could be prepared in a single production line thus making the costs of production comparable to the costs of a single recombinant protein.

This goal has been achieved through two tasks:

I) Exploring the limits of the carrier-based method for the production of recombinant peptides by preparing fusion proteins bearing two or more AMP modules fused at the C-terminus of ONC-DCless-H6, according to the schemes:

ONC-DCless-H6-X-CAMP₁-X-CAMP₂

&

ONC-DCless-H6-(X-AAMP-X-CAMP)_n

II) Preparing “**carrier-less modular artificial precursors**” that can be efficiently expressed in a bacterial host and successively cleaved to give an AMP mixture according to the scheme:

(AAMP-X-CAMP-X-)_n-TAG

where “TAG” is a short tag sequence or an AMP that can be used as a tag sequence during the purification procedure.

Chapter 2-Materials and Methods

2.1 Materials

Expression host strain *E. coli* BL21(DE3) genotype: 95 F⁻ *ompT hsdSB* (rB-mB -) *gal dcmrne* 131 (DE3) and plasmid pET22b(+) were purchased from Novagen (San

Diego, CA, USA). *E. coli* strain TOP10F⁺ was obtained from Invitrogen (San Diego, CA, USA). QIAprep spin miniprep kit was from Qiagen (Germantown, MD, USA). Wizard SV.Gel and PCR Clean-Up DNA Purification System for elution of DNA fragments from agarose gel was purchased from Promega (Madison, WI, USA). Enzymes and other reagents for DNA manipulation were from New England Biolabs (Ipswich, MA, USA). Ni Sepharose™ 6 Fast Flow was from GE Healthcare (Uppsala, Sweden). Yeast extract was from Becton-Dickenson (Franklin Lakes, NJ). Trypton was purchased from PanReac Applichem (Germany, UE). All other chemicals were from Sigma- Aldrich (Milano, Italy).

2.2 General procedures

Bacterial cultures, plasmid purifications and DNA manipulation were carried out according to Sambrook [43]. DNA sequences and oligonucleotide synthesis were performed by Eurofins MWG Operon service (Ebersberg, Germany). Sodium Dodecyl Sulphate PolyAcrylamide Gel Electrophoresis (SDS-PAGE) was carried out according to Laemmli [44]. The percentage of polyacrylamide was 6% for the stacking gel and 15% (to separate proteins with a molecular weight up to 10'000 Da) or 20% (to separate peptides with molecular weight lower than 8'000 Da) in the resolving gel. Cleavage efficiency was analyzed by SDS-PAGE 20%. Gels were stained by Coomassie Blue staining solution containing 4% (v/v) formaldehyde to cross-link proteins and polypeptides [45]. *Gallus gallus* lysozyme (14.3 kDa) and colorburst electrophoresis marker (Sigma-Aldrich, St. Louis, MO, USA) were used as molecular marker. When appropriate, the relative amount of bands was determined by densitometry performed using the Gel Doc™ XR system (Bio-Rad Laboratories, Inc.) equipped with the Quantity One Software. Protein concentration were determined using the Bradford Protein Assay (Sigma-Aldrich, St. Louis, MO, USA) with standard curves generated using bovine serum albumin. Concentrations of purified fusion proteins and peptides were determined by spectrophotometric analysis using the extinction coefficients calculated using the ProtParam tool (accessible to the address <http://web.expasy.org/protparam/>). Alternatively, Bicinchoninic acid Assay was used for peptides without aromatic residues.

2.3 Synthetic coding sequences

Synthetic DNA coding for the recombinant proteins described in “Results and discussion” section were obtained either from Eurofin Genomics (Ebersberg, Germany) or GenScript (Piscataway, USA).

2.4 Bacterial growth culture media

Luria Bertani Broth (LB) contained 1 % (w/v) sodium chloride, 1% (w/v) trypton and

0.5 % (w/v) yeast extract. The solid medium was obtained from the liquid one by adding agar to a final concentration of 1.5% (w/v) as a gelling agent [43].

Terrific Broth (TB) was prepared with 1.2 % (w/v) trypton, 2.4 % (w/v) yeast extract;

0.4 % (v/v) glycerol and potassium phosphate buffer 89 mM pH 7.4.

2.5 Antibiotics

Ampicillin (Amp) was used always at a concentration of 100 µg/mL.

2.6 Expression of recombinant proteins

E. coli strain BL21(DE3) was used to express all the recombinant proteins. Cells, transformed with pET recombinant plasmids were grown in 10 mL of TB medium containing 100 µg/ml ampicillin, at 37°C up to an absorbance of 2 OD at 600 nm. These cultures were used to inoculate 1 L of TB/ampicillin medium supplemented with 4 g/L glucose. Cultures were incubated at 37°C up to OD_{λ600nm} of 3.5-4. Expression of recombinant proteins was induced by addition isopropyl-β-D-thiogalactopyranoside (IPTG) at a final concentration of 0.4 mM.

Cells were harvested after overnight induction by centrifugation at 8000x g for 15 min at 4°C and washed with 50 mM Tris-HCl buffer, pH 7.4. The bacterial pellet was suspended in 100 mM Tris-HCl, pH 7.4, containing 20 mM EDTA, and sonicated in a cell disruptor (10 x 1 min cycle, on ice). The suspension was then centrifuged at 18,000 x g for 60 min at 4°C. Soluble and insoluble fractions were analyzed by SDS- PAGE.

Only in the case of ONC-DCless-H6-(P)PAP-A3, ONC-DCless-H6-(P)PAP-A3(Pro26) and ONC-AT2H the insoluble fractions containing the recombinant protein in the form of inclusion bodies were washed three times in 0.1 M Tris-HCl, pH 7.4, containing 10 mM EDTA, 2% Triton X-100 and 2 M urea, followed by repeated washes in 0.1 M Tris-HCl, pH 7.4, to eliminate traces of Triton, urea and EDTA.

2.7 Purification of fusion proteins

All the proteins were purified by immobilized metal ion affinity chromatography (IMAC), using the Ni Sepharose™ 6 Fast Flow resin. An amount of inclusion bodies corresponding to about 100 mg of fusion proteins were dissolved in 10 mL of denaturing buffer (5 M guanidine/HCl in 100 mM Tris-HCl, pH 7.4) and incubated on a rotary shaker at 37°C for 3 h under nitrogen atmosphere. Soluble fractions were collected by centrifugation and incubated with 5 mL of Ni Sepharose™ 6 Fast Flow resin equilibrated in denaturing buffer. The resin was shaken at 4°C for 3 h and then collected by centrifugation. The supernatant, containing the unbound proteins, was discarded. The resin was washed three times with 25 ml of denaturing buffer at 4°C for 30 min and then packed in a glass column. Only in the case of ONC-AT2H, the resin was first packed in a glass column and then washed three times with 25 ml of denaturing buffer and 5 mM imidazole. The fusion proteins were eluted with 20 ml of 0.1 M sodium acetate buffer, pH 5.0, containing 5 M guanidine/HCl (elution buffer). The eluate was extensively dialyzed against 0.1 M acetic acid at 4°C. Purified fusion protein concentrations were determined by spectrophotometric analysis using theoretical extinction coefficients calculated using the ProtParam tool.

2.8 Acid cleavage of Asp-Pro peptide bond

Routinely acid cleavage of fusion proteins was performed in 0.1 M acetic acid buffered at pH 2.0 by addition of HCl for 24 h at 60°C in a water bath under nitrogen atmosphere. Percentage of cleaved protein was determined by densitometric analysis of SDS-PAGE gels as described in "General procedures".

2.9 Purification of recombinant peptides

After acid cleavage of the fusion proteins containing the carrier ONC-DCless-H6, the pH of the peptide mixtures was adjusted to 7–7.2 by adding aqueous NH₃. Samples were purged with N₂ and incubated at 28°C for 16 h in a water bath. Soluble peptides were isolated from the insoluble carrier through repeated cycles of centrifugation at 18,000 x g for 60 min at 4°C. Purified peptides were lyophilized and stored at -80°C. Peptide concentrations were determined by spectrophotometrically using the theoretical extinction coefficients calculated using the ProtParam tool or by the BCA assay. Peptides derived from the cleavage of PAP-A3(Pro26) and ONC-AT2H were purified by RP-HPLC as described in section 2.10. Purity of peptides was determined by SDS-PAGE and by RP-HPLC as described in section 2.10.

2.10 RP-HPLC

RP-HPLC (Reverse-phase high performance liquid chromatography) analyses were performed on a Jasco LC-4000 system equipped with PU-4086 semi-preparative pumps and MD-4010 photo diode array detector. Jupiter 5μ C18 300Å column (250 x 4,6 mm, 5μm particle size) provided by Phenomenex was used for analytical chromatographies. Peptide purifications were carried out on Europa Protein 300 C18 column (5μm, 25 x 1mm) from Teknokroma. Solvents were 0.05% trifluoroacetic acid (TFA) in water (solvent A) and 0.05% TFA in acetonitrile (solvent B).

Pepsinogen and its fragments were analysed on the Jupiter 5μ C18 300A column by gradient 1 (5% solvent B for 10 min, 5-20% solvent B in 5 min, 20-30% solvent B in 40 min, 30-40% solvent B in 5 min, 40-95% solvent B in 5 min). Elution profiles were recorded at 280 nm at a flow rate of 1 ml/min.

(P)IMY25 and (P)FLK22 peptides were purified on the Europa Protein 300 C18 column by gradient 2 (5% solvent B for 10 min, 5-20% solvent B in 5 min, 20-30% solvent B in 85 min, 30-95% solvent B in 1 min). Elution profiles were recorded at 280 nm at a flow rate of 2 ml/min.

Purified AT2H recombinant fusion protein and its hydrolysis pattern were analyzed on the Jupiter 5μ C18 300A column by gradient 3 (5% solvent B for 10 min, 5-30% solvent B in 5 min, 30-46% solvent B in 80 min, 46-100% solvent B in 5 min). Elution profiles were recorded at 230 nm at a flow rate of 1 ml/min.

(P)GKY21, FibA and HRP peptides were purified on the Europa Protein 300 C18 column by gradient 4 (5% solvent B for 10 min, 5-20% solvent B in 5 min, 20-36% solvent B in 85 min, 36-100% solvent B in 1 min). Elution profiles were recorded at 230 nm at a flow rate of 2.5 ml/min.

2.11 Antibacterial and antibiofilm assay

Antibacterial activity assays were carried out by i) agar dilution plate viable-count method [46] and ii) by broth microdilution method to determine the Minimal Inhibitory Concentration (MIC) with the collaboration of Dr. Katia Pane (Department of Biology, University of Naples, Federico II) [47]. The minimal inhibitory concentration was defined as the lowest concentration completely inhibiting cell growth. Routinely assays were performed in Nutrient broth 0.5X.

i) *E. coli* strain ATCC25922 was used in the antibacterial tests. The bacteria were grown for 3 h, diluted 1 : 1000 in 10 mM MOPS buffer (pH 6.9), and incubated with increasing concentrations of peptides mixture at a density of 4.4×10^7 colony-forming units (CFUs) in 1 mL. After 2 h at 37 °C, serial dilutions of each protein–bacteria mix were prepared and plated, and CFUs remaining after each treatment

were determined. For each experiment, triplicate assays were performed.

ii) Assays were carried out in Difco Nutrient Broth composed of 0.5% beef extract (w/v),

0.05% pepton and 0.25% NaCl, using sterile 96-well polypropylene microtiter plates (cat. 3879, Costar Corp., Cambridge, MA). Twofold serial dilutions of peptides were carried out in the test wells to obtain concentrations ranging from 100 μ M to 0.2 μ M. Bacteria were inoculated from an overnight culture at a final concentration of $\sim 5 \times 10^5$ CFU/mL per well and incubated overnight at 37°C. MIC value was taken as the lowest concentration at which growth was inhibited. Three independent experiments were performed for each MIC value.

Antibiofilm assays were performed in collaboration with the groups of Dr. Eliana De Gregorio and Prof. Maria Rosaria Catania (Dipartimento di Medicina molecolare e Biotecnologie mediche, Università degli Studi di Napoli Federico II).

Antibiofilm activity was measured by crystal violet staining of adherent biofilm in BM2 minimal medium in 96-well plates to obtain the Minimal Biofilm Inhibitory Concentrations leading to 50% (MBIC₅₀) or 100% (MBIC₁₀₀) decrease in static biofilm growth.

2.12 Bacterial strains used for antimicrobial susceptibility test

Strains included *Escherichia coli* ATCC35218, *Enterococcus faecalis* ATCC29212, *Acinetobacter baumannii* ATCC17878, *Klebsiella pneumoniae* ATCC 700603, *Escherichia coli* ATCC25922 (kindly provided by Dr. Eliana De Gregorio, University of Naples, Federico II), *Salmonella enterica* serovar *typhimurium* ATCC14028, *Salmonella enteritidis* 706 RIVM (kindly provided by Dr. Edwin Veldhuizen, University of Utrecht, Holland), *Pseudomonas aeruginosa* PAO1 wild type (kindly provided by Dr. Donatella de Pascale, CNR, Naples), *Staphylococcus aureus* MRSA clinical isolate, *Bacillus subtilis* subsp. *spizizenii* ATCC6633, *Pseudomonas aeruginosa* ATCC27853, *Bacillus spizizenii* ATCC6633 (kindly provided by Dr. Edwin Veldhuizen, University of Utrecht, Holland).

2.13 Mass Spectrometry

Mass spectrometry analyses were performed on a MALDI micro MX™, matrix-assisted laser desorption/ionization time-of-flight mass spectrometer (MALDI-TOF MS), (Waters, Milford, MA USA).

For MALDI-TOF analysis, 1 μ L of digestion mixtures or each peptide solution was mixed with 1 μ L of saturated α -cyano-4-hydroxycinnamic acid matrix solution [10 mg/mL in acetonitrile:0.1% TFA (1:1; v/v)]. Thus, a droplet of the resulting mixture (1 μ L) was placed on the mass spectrometer's sample target and dried at room temperature. Once the liquid was completely evaporated, samples were loaded into the mass spectrometer and analysed. The instrument was externally calibrated using a tryptic alcohol dehydrogenase digest (Waters, Manchester, UK) in reflectron mode. For linear mode, a four-point external calibration was applied using an appropriate mixture (10 pmol/mL) of insulin, cytochrome C, horse Mb and trypsinogen as standard proteins (Sigma). A mass accuracy near to the nominal (50 and 300 ppm in reflectron and linear modes, respectively), was achieved for each standard.

All spectra were processed and analysed using MassLynx 4.1 software [48].

Chapter 3-Results and Discussion

3.1 Production of CAMPS derived from the activation peptide of human pepsinogen.

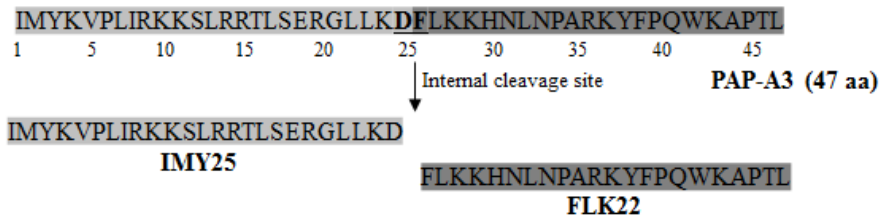
In order to verify the possibility to prepare ONC based fusion proteins bearing more than one CAMP module, the activation peptide of isoform A3 of human pepsinogen (PAP-A3) was selected as test CAMP. Pepsinogen is the precursor of pepsin, the main protease of gastric juice. With respect to pepsin it contains at the N-terminus an additional sequence of 47 residues, the so-called activation peptide, which is essential for pepsinogen storage in the secretory granules and for secretion process. Once pepsinogen is secreted in the gastric lumen, pepsin itself remove the activation peptide by a single cleavage between residue 47 and 48 of pepsinogen. According to literature, once released, activation peptide has no other physiological role. However, the activation peptide has been identified as a potential CAMP by a novel bioinformatic tool allowing the identification of cryptic antimicrobial peptides developed by our research group and recently accepted for publication in Journal of Theoretical Biology [49]. As the activation peptide is 47 residues long, at the beginning of the present project it was the longest peptide selected for the expression as a fusion protein with the carrier ONC-DCless-H6. Furthermore, the bioinformatic tool also suggested the presence of two shorter putative CAMPs within the activation peptide, approximately corresponding to the first 20-24 and the last 22 residues of the peptide. Intriguingly, it has been reported that activation peptide is, at least in part, cleaved by pepsin itself between residues D25-F26 [50] thus releasing the two hypothetical short CAMPs. Therefore, PAP-A3 can be considered a natural example of CAMPs present in tandem in a precursor thus being an ideal candidate to verify the possibility to express and purify several AMPs starting from the same precursor. It should be noted that PAP-A3 already contains an aspartate residue exactly at the predicted boundary between the two modules (i.e. bond D25-F26). Therefore, by simply inserting a proline residue between residue D25 and residue F26 in the PAP-A3 sequence it is possible to obtain a precursor containing an acidic cleavage site (sequence LLKDPFLK) located at the boundary between the two hypothetical CAMP-like modules (Fig. 3.1).

Accordingly, two recombinant fusion proteins, ONC-DCless-H6-(P)PAP-A3 and ONC-DCless-H6-(P)PAP-A3(Pro26) were prepared, which differ for the presence of an additional proline in the latter protein (Fig. 3.1).

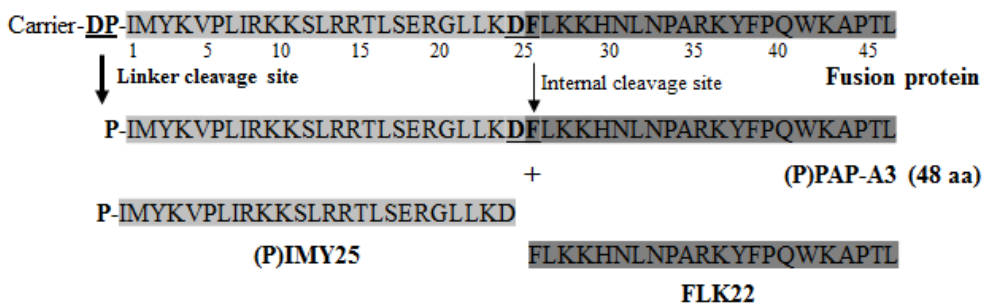
The acidic hydrolysis at 60°C of ONC-DCless-H6-(P)PAP-A3 should produce two main fragments, the onconase carrier and the recombinant activation peptide with an additional proline at the N-terminus left by the acidic cleavage, herein called (P)PAP-A3. As also the sequence D25-F26, present in PAP-A3, could undergo acidic hydrolysis at very low efficiency, the two main fragments could possibly be contaminated by two minor fragments corresponding to the first 26 residues of (P)PAP-A3 [peptide (P)IMY25] and the last 22 residues of (P)PAP-A3 [peptide FLK22] (Fig. 3.1). On the other hand the acidic hydrolysis of ONC-DCless-H6-(P)PAP-A3(Pro26) should produce three main fragments: (i) onconase, (ii) the first 25 residues of PAP-A3 [i.e. (P)IMY25] and (iii) the last 22 residue of PAP-A3 with an additional proline at the N-terminus [herein called (P)FLK22].

The desired open reading frames were prepared by a cassette mutagenesis strategy routinely used in our laboratory. Briefly, the synthetic sequences coding for (P)PAP-A3 and (P)PAP-A3(Pro26) peptides were obtained by MWG-Biotech AG (Ebersberg, Germany) and cloned into pET22b(+)/ONC-DCless-H6 vector coding for the optimized ONC carrier.

A Natural peptides



B Peptides derived from ONC-DCless-H6-(P)PAP-A3 fusion protein



C Peptides derived from ONC-DCless-H6-(P)PAP-A3(Pro26) fusion protein

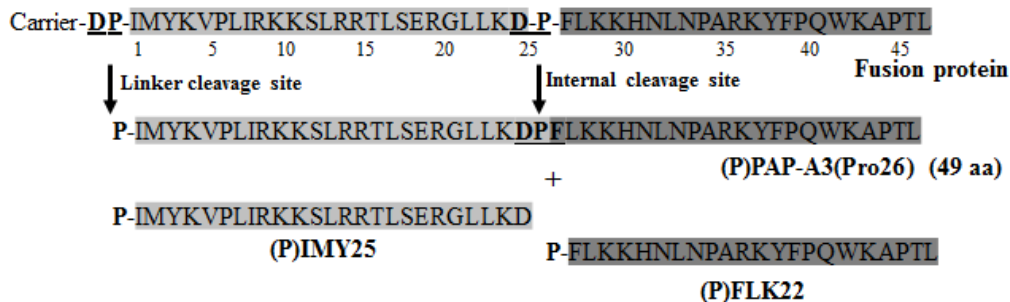


Figure 3.1. Natural and recombinant peptides derived from human pepsinogen A3 activation peptide. A) Full length pepsinogen activation peptide and its two shorter peptides derived from cleavage of DF internal acid labile site (bold and underlined characters) into the acid stomach environment. B) Recombinant peptides derived from ONC-DCless-H6-(P)PAP-A3 fusion protein by cleavage of DP site into the protein linker region [(P)PAP-A3 peptide] and DF internal cleavage site [(P)IMY25 and FLK22 peptides]. C) Recombinant peptides derived from ONC-DCless-H6-(P)PAP-A3(Pro26) fusion protein by cleavage of DP site into the protein linker region [(P)PAP-A3(Pro26) peptide] and DPF internal cleavage site [(P)IMY25 and (P)FLK22 peptides]. Internal cleavage sites were highlighted as bold and underlined characters.

The recombinant proteins were expressed in *E. coli* strain BL21(DE3) as inclusion bodies at very high levels (about 200-250 mg/L in Terrific broth) (Fig. 3.2). Purification by immobilized metal ion affinity chromatography (IMAC) followed by dialysis in acetic acid 0.1 M, allowed a recovery of about 95% of the fusion proteins with about 98% purity (Fig. 3.3). Release of peptides from recombinant proteins was obtained by chemical cleavage of DP sequences in acidic medium (pH 2). As shown by SDS-PAGE analysis (Fig. 3.4), after 24 h of incubation at 60°C, the DP sequence located into the linker region of both fusion proteins, was efficiently cleaved (about 95% efficiency). Peptides were purified from the carrier by selective precipitation of the carrier at pH 7.2, followed by repeated cycles of centrifugation. Peptides were recovered in the soluble fraction at neutral pH, whereas carriers were found in the insoluble fractions. Two peptide bands were observed from the cleavage of both recombinant proteins (Fig. 3.4).

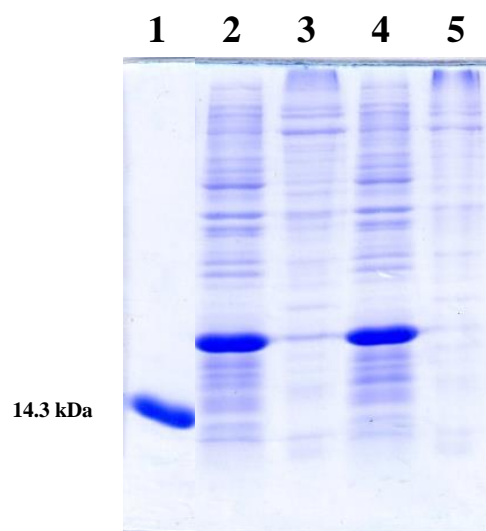


Figure 3.2. Expression of recombinant proteins. SDS-PAGE (15%) analysis of fusion proteins. Lane 1: *Gallus gallus* lysozyme; lane 2-4: insoluble fractions after cell lysis of cultures expressing ONC-DCless-H6-(P)PAP-A3 and ONC-DCless-H6-(P)PAP-A3(Pro26) fusion proteins, respectively; lane 3-5: soluble fractions after cell lysis of cultures expressing ONC-DCless-H6-(P)PAP-A3 and ONC-DCless-H6-(P)PAP-A3(Pro26) fusion proteins, respectively.

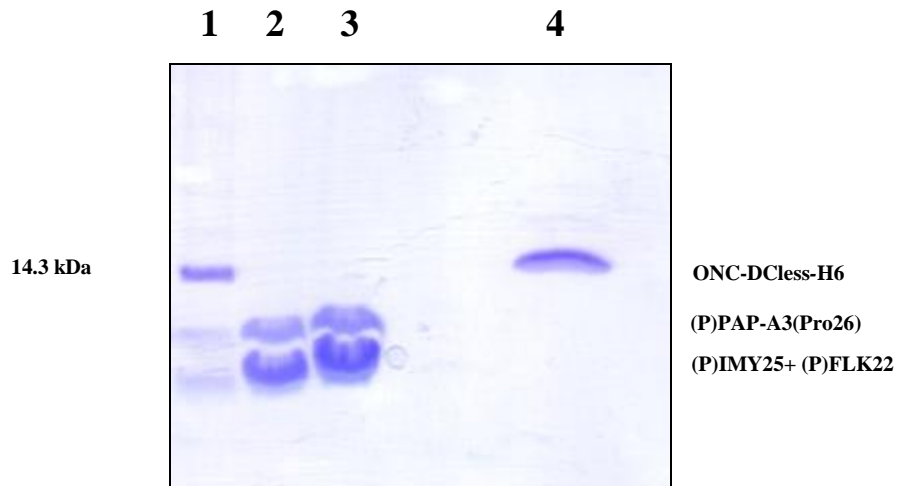


Figure 3.3. Hydrolysis analyses of recombinant proteins.

ONC-DCless-H6-(P)PAP-A3(Pro26) fusion protein; lane 1: *Gallus gallus* lysozyme (14.3 kDa), purified (P)PAP-A3 (5.792 kDa) and (P)IMY25 (3.111 kDa) peptides (acid cleavage pattern); lane 2: soluble fraction after neutralization at pH 7; lane 3: soluble fraction after neutralization at pH 7; lane 4: insoluble fraction after neutralization at pH 7 (carrier protein and uncleaved fusion protein). Gels (20 %) were stained by Coomassie Brilliant Blue R-250 in the presence of 4% formaldehyde.

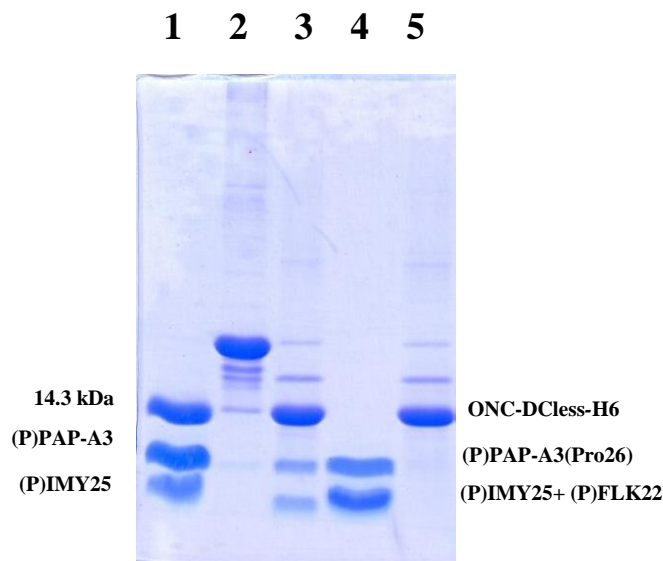


Figure 3.4. Hydrolysis pattern analyses of recombinant proteins by SDS-PAGE.

ONC-DCless-H6-(P)PAP-A3(Pro26) fusion protein; lane 1: *Gallus gallus* lysozyme (14.3 kDa), purified (P)PAP-A3 (5.792 kDa) and (P)IMY25 (3.111 kDa) peptides; lane 2: purified fusion protein after dialysis; lane 3: acid cleavage pattern; lane 4: soluble fraction after neutralization at pH 7; lane 5: insoluble fraction after neutralization at pH 7 (carrier protein and uncleaved fusion protein). Gels (20 %) were stained by Coomassie Brilliant Blue R-250 in the presence of 4% formaldehyde.

The two hydrolysis mixtures were analyzed by RP-HPLC (Fig. 3.5) and mass spectrometry (Fig. 3.6) which allowed to identify all the expected fragments. In the case of ONC-DCless-H6-(P)PAP-A3 the main peak in the HPLC chromatogram corresponded to (P)PAP-A3 whereas two small peaks eluting earlier showed mass values identical to those expected for peptides (P)IMY25 and FLK22 within the experimental error. From the densitometric analysis of the Coomassie stained gels and the relative areas of the peaks in the HPLC chromatogram it could be estimated that about 95% of the ONC-DCless-H6-(P)PAP-A3 fusion protein (Fig. 3.1B) was cleaved at Asp-Pro site at the N-terminus of PAP-A3 and about 5% of the peptide was cleaved at Asp25-Phe26. These percentages are in agreement with the previously determined average cleavage frequencies of Asp-Pro and Asp-X sequences and show that the desired peptide of 47 residues can be obtained with a minimal loss due to the fragmentation at the inner aspartate residue.

In the case of ONC-DCless-H6-(P)PAP-A3(Pro26) the three expected peptides (P)PAP-A3(Pro26), (P)IMY25 and (P)FLK22 were identified. However, the quantitative analysis allowed to estimate that about 95% of the ONC-DCless-H6-(P)PAP-A3(Pro26) fusion protein (Fig. 3.1B) was cleaved at Asp-Pro site at the N-terminus of PAP-A3 and only about 80% of the peptide was further cleaved at the inner site Asp25-Pro26. The lower cleavage efficiency of Asp25-Pro26 site compared to the Asp-Pro sequence in the linker region is likely due to a higher steric hindrance of the surrounding sequences as shown in the alignment below:

GTG**DP**IMY
LLK**DP**FLK

The presence of the flexible linker (GTG) upstream the Asp-Pro site at the N-terminus is likely useful for a high efficient cleavage.

In order to increase cleavage efficiency, the acidic cleavage was performed in the presence of denaturants or at temperatures higher than 60°C. Unfortunately, hydrolysis in the presence of 4 M guanidine did not improve the efficiency, whereas, hydrolysis carried out at 70°C for 24 h greatly increased cleavage efficiency but also yielded unwanted unspecific fragmentation of the carrier and/or of the peptides. Therefore, the previously optimized cleavage conditions (0.1 M acetic acid pH 2, at 60°C for 24 h) were routinely used.

Peptides were purified by RP-HPLC with a recovery of about 70% (Fig. 3.7). Purity of peptides was found to be more than 95% as measured by RP-HPLC (Fig. 3.8). (P)PAP-A3 peptide was produced with a final yield of about 18-20 mg/L of culture, whereas the shorter fragments (P)IMY25 and (P)FLK22 were produced with a final yield of 7-8 mg/L of culture for each peptide. Therefore, in spite of the incomplete cleavage of the inner Asp-Pro our strategy proved to be suited for the combined production of the two recombinant peptides.

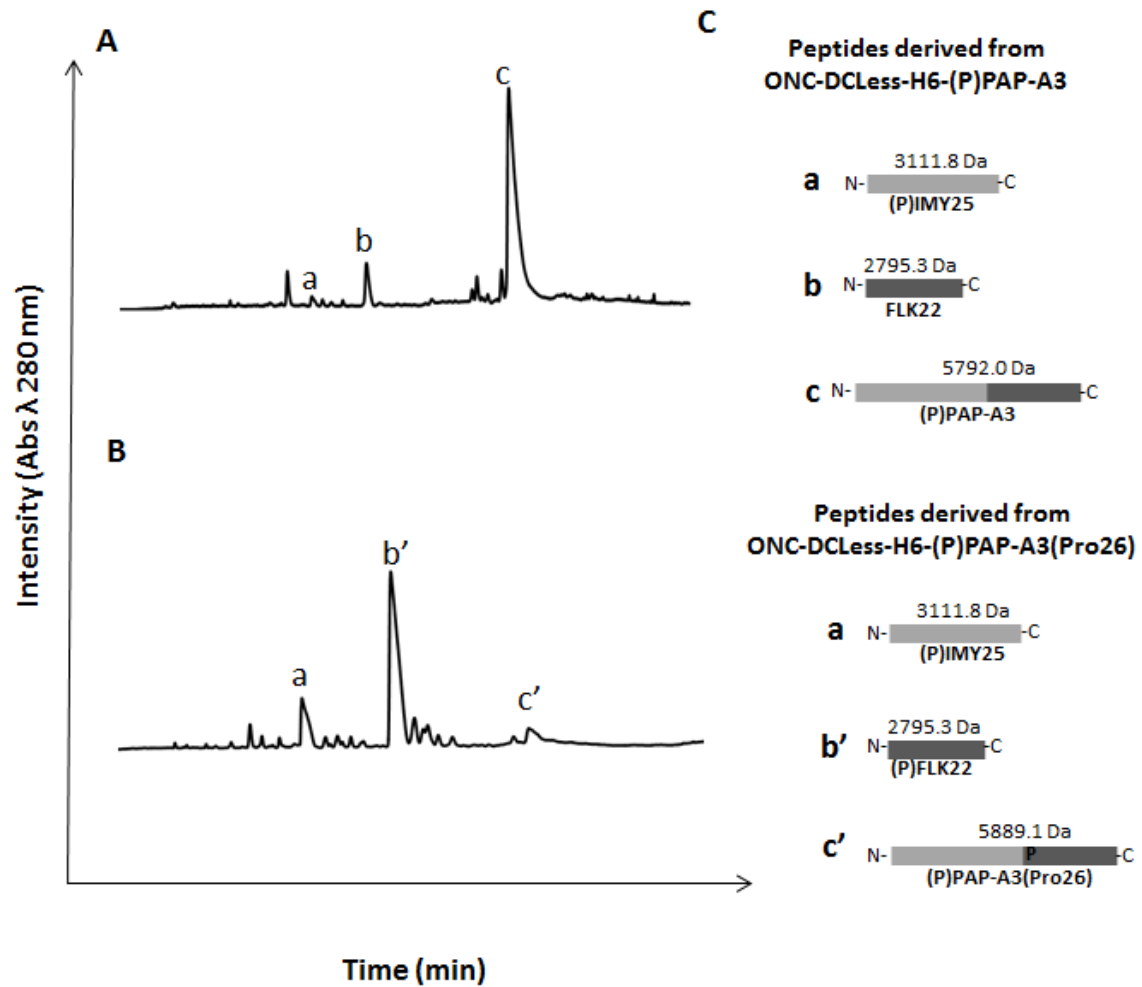


Figure 3.5. RP-HPLC analyses of peptide mixtures.

Samples were analyzed after selective carrier precipitation at neutral pH on Jupiter 5u C18 300A column. A) Peptides derived from cleavage of ONC-DCLess-H6-(P)PAP-A3 fusion protein; peak c, (P)PAP-A3 full length peptide; peaks a and b, the two shorter peptides [(P)IMY25 and FLK22, respectively] derived from cleavage of DF acid labile internal site. B) Peptides derived from cleavage of ONC-DCLess-H6-(P)PAP-A3(Pro26) fusion protein; peak c', (P)PAP-A3(Pro26) full length peptide; peaks a and b', the two shorter peptides [(P)IMY25 and (P)FLK22, respectively] derived from cleavage of DPF acid labile internal site. Molecular weight of peptides determined by Mass spectrometry were reported on the chromatograms. C) Representation of all recombinant peptides and their theoretical molecular weights.

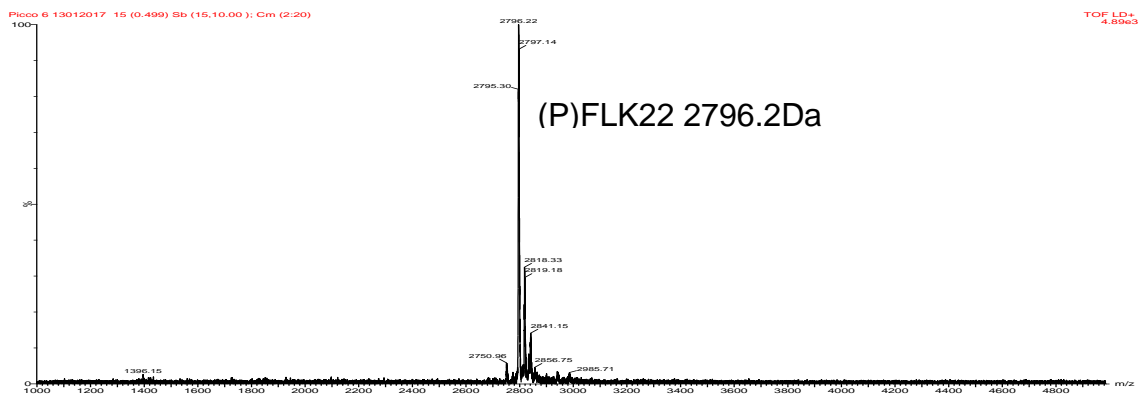
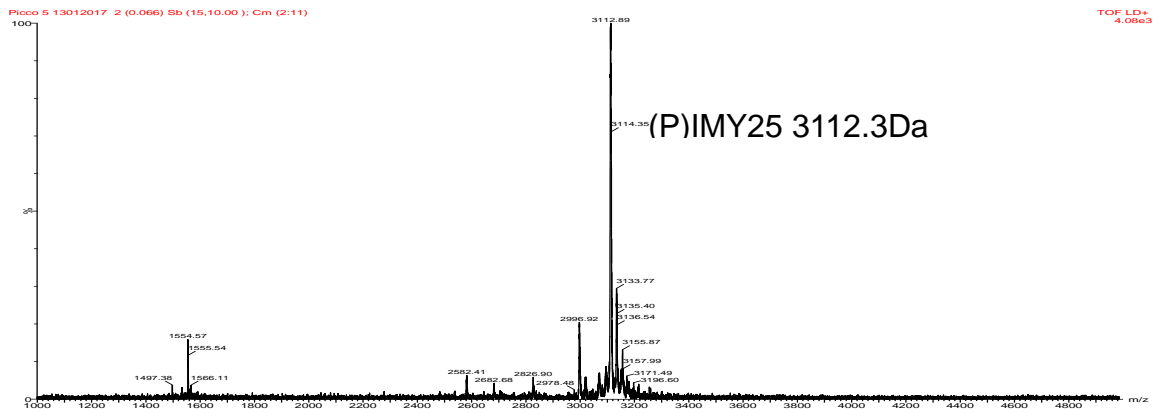
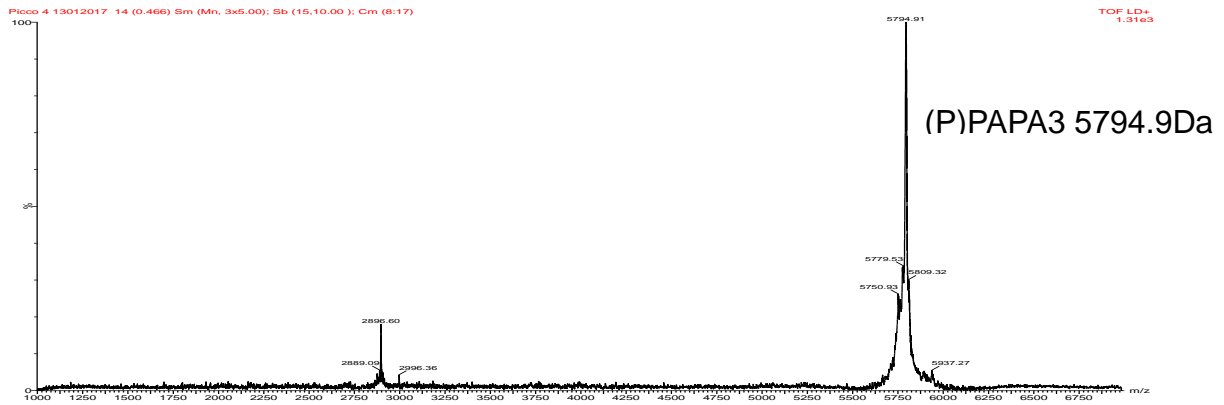


Figure 3.6. Mass spectrometry analysis.

In the table shows the experimental weight of the peaks obtained by mass spectrometry.

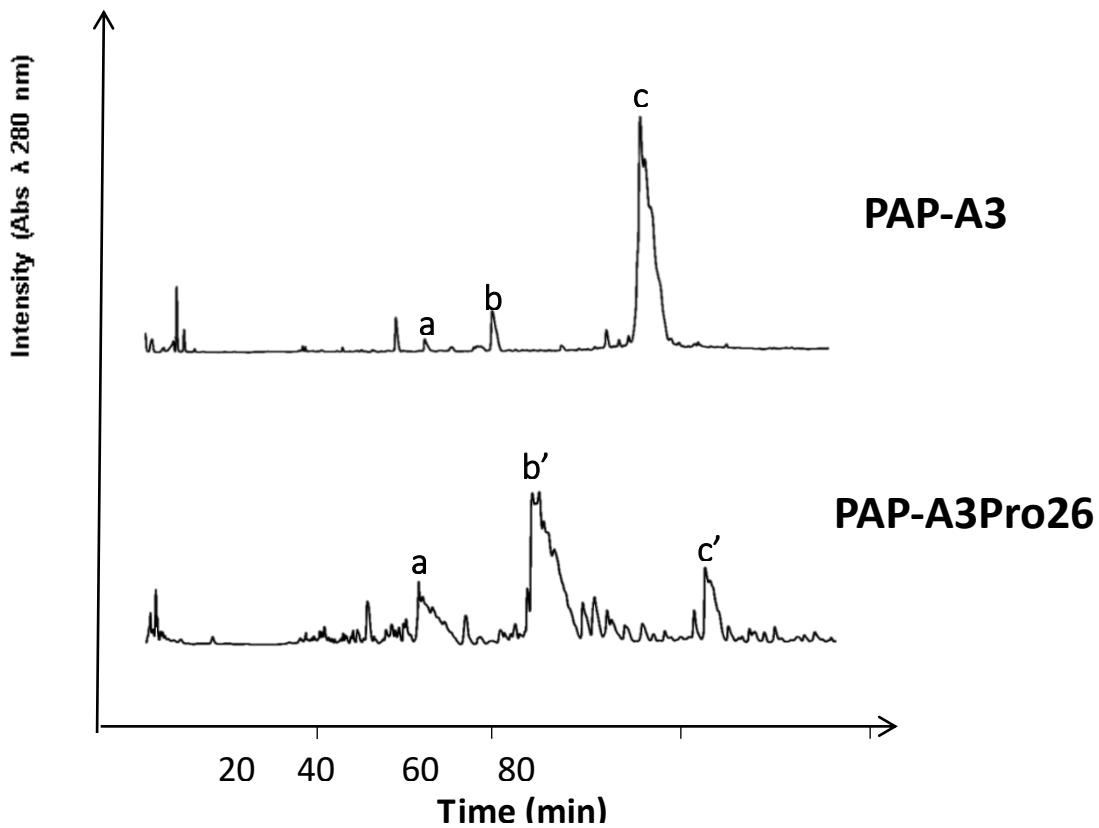


Figure 3.7. Peptide purifications by RP-HPLC.

Peptides were purified on Europa Protein 300 C18 column. A) Peptides derived from cleavage of ONC-DCLess-H6-(P)PAP-A3 fusion protein; peak c, (P)PAP-A3 full length peptide; peaks a and b, the two shorter peptides [(P)IMY25 and FLK22, respectively] derived from cleavage of DF acid labile internal site. B) Peptides derived from cleavage of ONC-DCLess-H6-(P)PAP-A3(Pro26) fusion protein; peak c', (P)PAP-A3(Pro26) full length peptide; peaks a and b', the two shorter peptides [(P)IMY25 and (P)FLK22, respectively] derived from cleavage of DPF acid labile internal site.

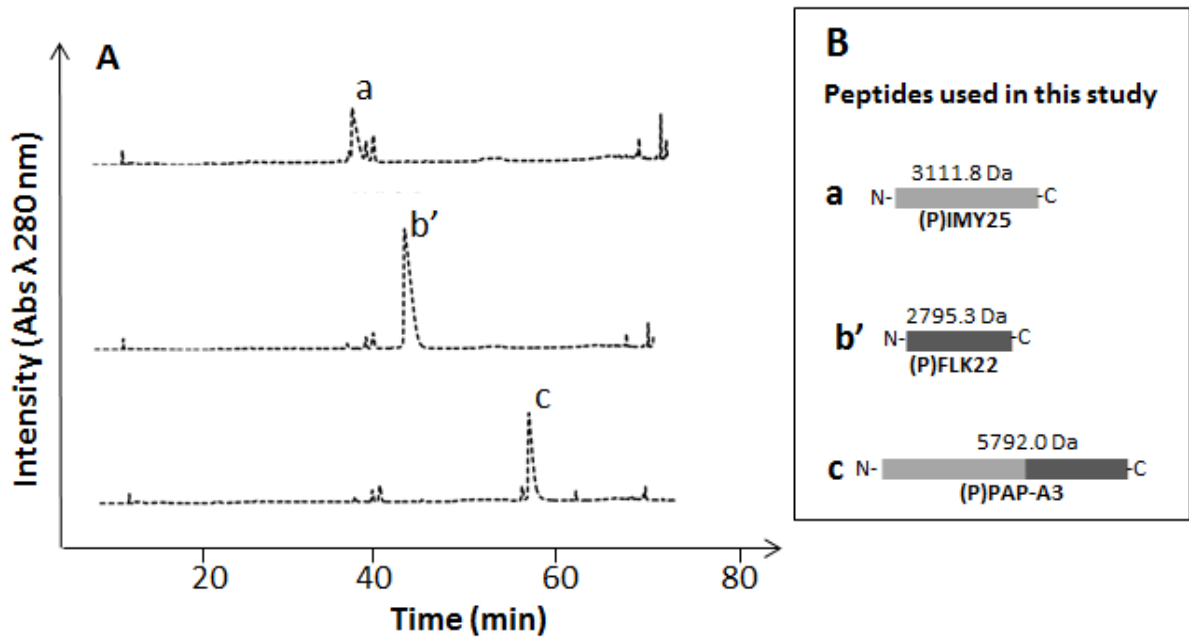


Figure 3.8. Purity analyses by RP-HPLC of recombinant peptides tested as CAMPs in this study. Samples were analyzed on Jupiter 5u C18 300A after RP-HPLC purification. A) Peaks a and b', shorter peptides [(P)IMY22 and (P)FLK22, respectively] derived from cleavage of ONC-DCLess-H6-(P)PAP-A3(Pro26) fusion protein; peak c, (P)PAP-A3 full length peptide derived from cleavage of ONC-DCLess-H6-(P)PAP-A3 fusion protein. B) Representation of recombinant peptides and their theoretical molecular weights.

3.2 Antimicrobial activity

The antibacterial activity of peptides (P)PAP-A3, (P)IMY25 and (P)FLK22 was determined on the planktonic form of several Gram negative and Gram positive bacteria using as positive control (P)GKY20, a well known cryptic CAMP deriving from the C-terminus of human thrombin. An equimolar mixture of (P)IMY25 and (P)FLK22 (1µM of mixture corresponds to 1µM of (P)IMY25 plus 1µM of (P)FLK22), used to simulate a completely cleaved (P)PAP-A3(Pro26), was also assayed. As reported in Table 1 (P)PAP-A3 shows MIC values similar or even lower to those of the control peptide on all the strains except *P. aeruginosa* strains. As for the shorter fragments, only (P)IMY25 shows significant activity whereas (P)FLK22 is active only on two strains. Not surprisingly the mixture of (P)IMY25 and (P)FLK22 has an activity comparable to that of (P)IMY25 alone.

Table 1: Antibacterial activity of the recombinant pepsinogen A3 derived peptides. Assays were carried out by broth dilution method in Nutrient Broth 0.5 X. MIC values shown are the highest obtained from three independent experiments.

	MIC (µM)				
	(P)PAP-A3	(P)IMY25	(P)FLK22	Mix ^a	(P)GKY20
Intestinal-associated bacteria					
<i>Escherichia coli</i> ATCC 35218	6.25	25	>50	25	6.25
<i>Enterococcus faecalis</i> ATCC29212	12.5	50	>50	50	12.5
<i>Salmonella enteritidis</i> 706RIVM	6.25	25	>50	50	12.5
<i>Listeria monocytogenes</i> clinical isolate ^b	>50	>50	>50	>50	25
<i>Salmonella typhimurium</i> ATCC14028	6.25	25	>50	12.5	6.25
Relevant biofilm-forming bacteria					
<i>Staphylococcus aureus</i> MRSA ^c	6.25	25	>50	25	12.5
<i>Pseudomonas aeruginosa</i> PAO1	>50	>50	>50	>50	25
<i>Pseudomonas aeruginosa</i> RP73 ^d	6.25	6.25	12.5	12.5	3.12
<i>Pseudomonas aeruginosa</i> AA2 ^d	>50	>50	>50	>50	>50
<i>Pseudomonas aeruginosa</i> KK27 ^d	>50	>50	>50	>50	25
Other bacteria					
<i>Acinetobacter baumannii</i> ATCC17878	1.56	– ^e	– ^e	– ^e	6.25
<i>Bacillus spizizenii</i> ATCC6633	12.5	– ^e	– ^e	– ^e	12.5
<i>Klebsiella pneumoniae</i> ATCC700603	6.25	– ^e	– ^e	– ^e	12.5
<i>Pseudomonas aeruginosa</i> ATCC27853	12.5	– ^e	– ^e	– ^e	12.5
<i>Staphylococcus aureus</i> ATCC6538P	5.5	10	>50	– ^e	ongoing

^a A mixture composed of (P)IMY25 and (P)FLK22 at equimolar concentration was assayed.

^b *Listeria monocytogenes* clinical isolate, kindly provided by Dr. Eliana de Gregorio, was assayed in Heart Infusion Broth 0.5X

^c Methicillin resistant *Staphylococcus aureus*, kindly provided by Prof. E. Veldhuizen.

^d Three *Pseudomonas aeruginosa* clinical isolates from cystic fibrosis patients, kindly provided by Prof. A. Bragonzi.

^e Not determined on these bacterial strains.

3.3 Antibiofilm assays

Since several pathogenic bacteria form biofilm we also investigated whether pepsinogen A3 derived peptides could affect preformed biofilm.

Biofilm is a community of cells embedded in a self-produced polymeric matrix. The extracellular matrix acts as a filter able to reduce the penetration of toxic molecules (like antibiotics and AMPs). Moreover, microbial cells growing in a biofilm are physiologically distinct from planktonic cells of the same organism and often are intrinsically more resistant to antimicrobials than planktonic cells. As a consequence, antimicrobial agents active on planktonic cells often are active on biofilms only at very high concentrations and sometimes are not active at all. The peculiar nature of a biofilm makes also difficult to study the effect of antimicrobial agents on the bacterial community. For example, an antimicrobial agent could kill the cells inside the biofilm without affecting the extracellular matrix and hence its macroscopic structure. On the contrary, other antimicrobial agents could induce the “disaggregation” of the cells without killing them (i.e. escape from the biofilm).

In order to discriminate between these different effects we used confocal microscopy coupled with a live(green)/dead(red) fluorescent staining of the cells. Assays were performed in collaboration with the groups of Dr. Eliana De Gregorio and Prof. Maria Rosaria Catania (Dipartimento di Medicina molecolare e Biotecnologie mediche, Università degli Studi di Napoli Federico II)

Figure 3.9 shows the effect of the three peptides on a biofilm of *Staphylococcus aureus* strain ATCC6538P grown in static conditions. As highlighted by the bright red color at 25-50 μM (P)IMY25 induce considerable cell killing. Confocal microscopy results were further confirmed by using a cell viability assay (Fig. 3.10). Indeed, (P)IMY25 at 51 μM reduced cell viability by 80% compared to untreated cells. As observed for other antimicrobials this concentration is about 20-50 times higher than the MIC value measured on the planktonic form of this strain. Peptide (P)FLK22, less active than (P)IMY25 on the planktonic form of this strain, at 50 μM shows only a modest antimicrobial activity. Surprisingly, (P)PAP-A3, whose MIC value on the planktonic form is identical to that of (P)IMY25, does not kill the cells in the biofilm even at highest concentration assayed. On the other hand, at low concentrations (7-15 μM) the longer peptide seems to be able to induce eradication of the biofilm as evidenced by the less bright green labeling and the presence of black spots. The inability to kill the cells inside the biofilm matrix could be related to the considerably higher molecular weight of (P)PAP-A3 with respect to its fragments. As discussed above the extracellular matrix is a very complex network of polymers including (acidic) polysaccharides and nucleic acid which could form an impenetrable filter for large molecules. Moreover several agents able to induce the disaggregation of biofilm have been described. For example some polyamines interact with the acidic polyanions in the biofilm matrix thus influencing its structure and inducing cell detachment. The group of R. Hancock discovered that some peculiar very short CAMPs induce cell detachment entering into the cells and influencing the transcriptional activity, thus acting as true signal molecules. Both mechanism could explain the activity of (P)PAP-A3 however, at the moment, we have not investigated the interaction of the peptide with polysaccharides and nucleic acids nor if the peptide can be cleaved to small fragment by bacterial proteases.

It is more difficult to explain why at higher concentrations (P)PAP-A3 seems to lose this ability. A simple explanation could be an aggregation process at high concentrations. However, it could be speculated that if fragments of the peptide

act as signal molecules, different levels of this hypothetical signal could induce different and even opposite effects.

Figure 3.11 shows the effect of (P)PAP-A3 and (P)IMY25 on a biofilm of *Pseudomonas aeruginosa* strain PAO1 grown in static conditions. The characterization of (P)FLK22, on this strain is still ongoing. Surprisingly, (P)PAP-A3 has no effect on the biofilm of this strain whereas (P)IMY25 induce a strong disaggregation of the biofilm when added at concentrations lower than 50 μM . It should be remembered that *Pseudomonas aeruginosa* PAO1 (a Gram negative) and *Staphylococcus aureus* ATCC6538P (a Gram positive) are very distant strains and both the chemical nature of their extracellular matrix and their ability to respond to signal molecules could be very different.

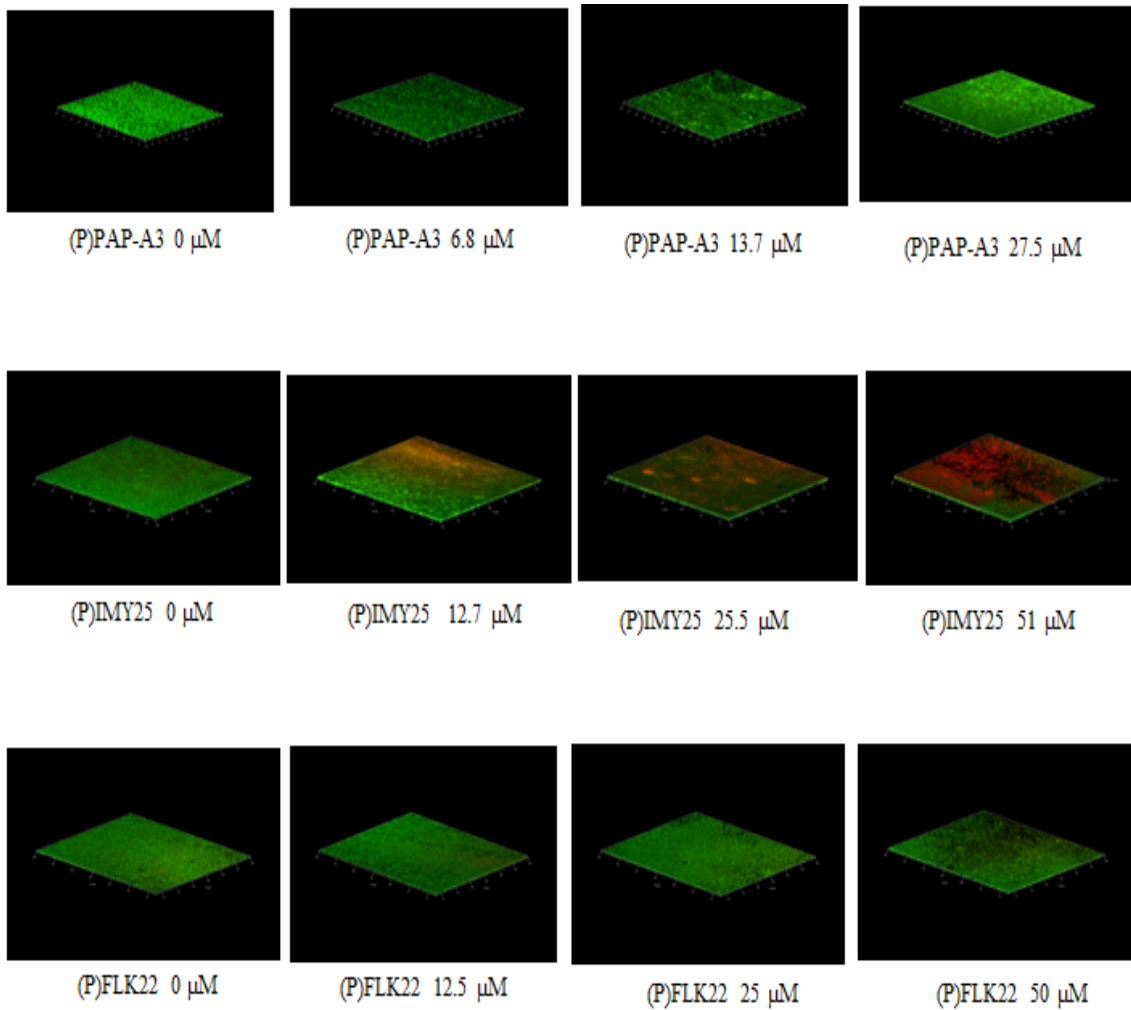


Figure 3.9. Confocal microscopy images of *S. aureus* ATCC 6538P static biofilm growth and eradication mediated by pepsinogen A3 derived peptides.

Images represents live cells stained with Syto-9 (green) whereas dead cells stained with Propidium iodide (red). The panels show representative results of at least two independent experiments.

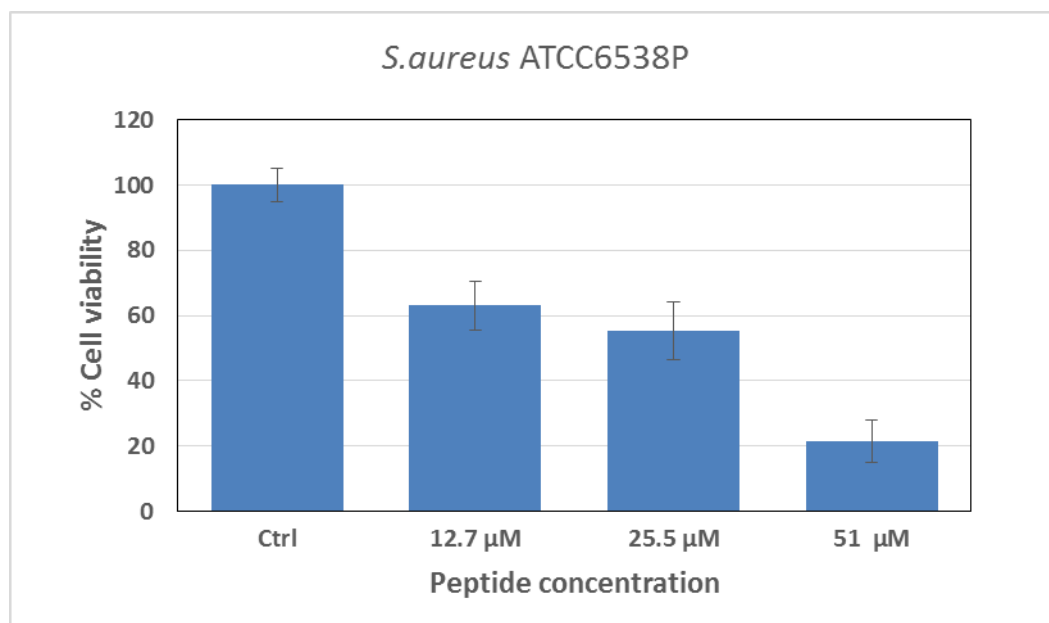


Figure 3.10. Cell viability assay on *S. aureus* ATCC6538P by XTT colorimetric assay. Cell viability was evaluated following static biofilm growth in glass chambers and peptides treatment.

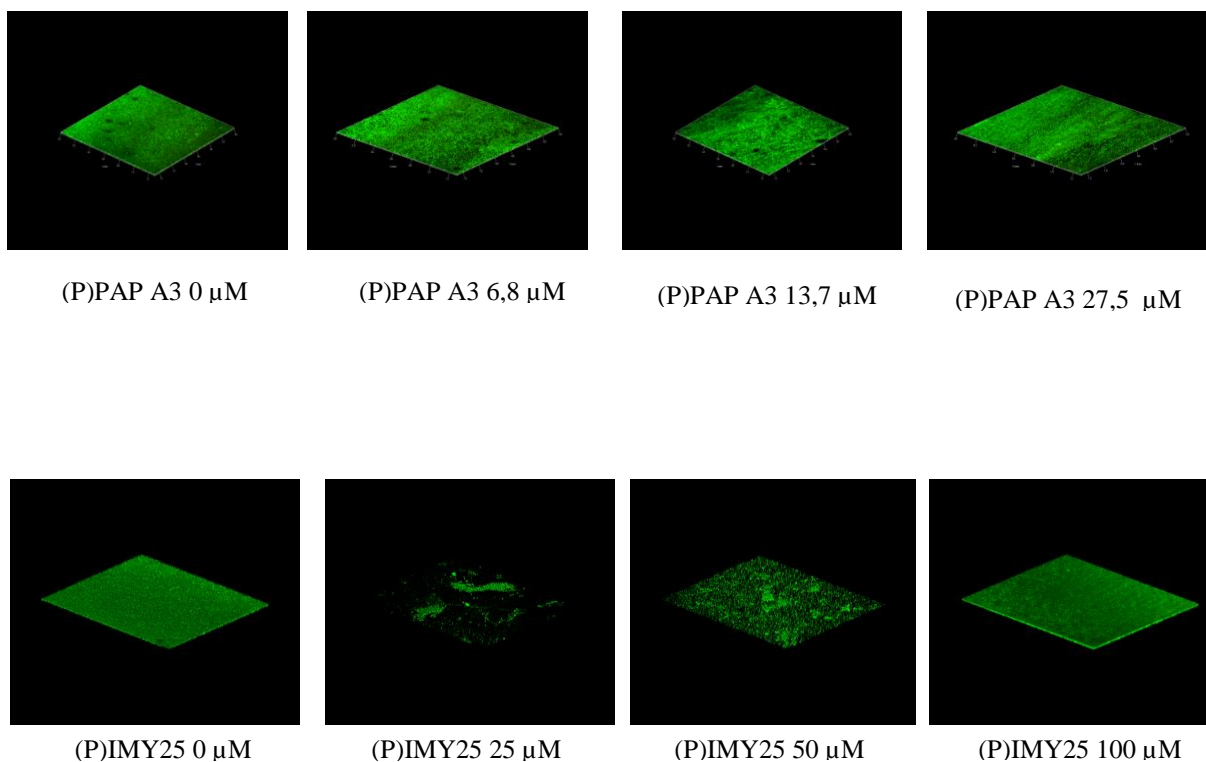


Figure 3.11. Confocal microscopy images of *PAO1* static biofilm growth and eradication mediated by pepsinogen A3 derived peptides.

Images represents live cells stained with Syto-9 (green) whereas dead cells stained with Propidium iodide (red). At 25 and 50 μM (P)IMY25 induced a significant reduction of the biofilm even if no dead (red) cells were observed thus indicating that it acts through the induction of detachment rather than by killing the cells. The panels show representative results of at least two independent experiments.

3.4 Designing of a carrier-less modular artificial precursor

The second objective of this PhD project is the optimization of the strategy initially developed by J. H. Lee [41] and described in the Introduction section. This requires the design of a modular artificial precursor containing alternate AAMP and CAMP modules which neutralize each other thus determining the formation of inclusion bodies or aggregates not harmful for the host. Such a precursor can be described by the general formula:



where “TAG” is a short tag allowing an easy purification of the precursor and DP are the acid labile sequences necessary for the cleavage of the precursor.

The success of this strategy requires a careful choice of the three type of modules. In particular the AAMP and the CAMP modules should have similar length and net charge so that each AAMP-DP-CAMP-DP unit is uncharged.

Among the possible CAMPs two promising candidates: GKY20, a CAMP derived from the C-terminus of human thrombin (20 aa; charge = +5) and ApoE-AP a CAMP derived from an internal domain of apolipoprotein E (18 aa; charge = +8) were selected. Both peptides have been expressed in our laboratory as ONC-DCless-H6 fusion proteins and purified with final yields of about 10-15 mg/L of culture and purity higher than 98%. Both GKY20 and ApoE-AP show high bactericidal activity on *P. aeruginosa* and *S. aureus*. Moreover, the two CAMPs can bind LPS and show anti-inflammatory activity.

Among the AAMPs described in literature, possible candidates were the fibrinopeptides A and B, the three SAAPs, dermcidin and thymosin-b4 (a platelet protein). On the basis of their chemical-physical features we selected fibrinopeptide A, FibA, as its length and charge density (16 aa; charge = -3;) are comparable to those of GKY20.

Taking into account the two aspartate residues of the cleavage sites, the unit FibA-DP-GKY20-DP has net charge = 0, therefore, this combination has been chosen for all the modular precursors.

As for the TAG module, in principle a peptide able both to perform the role of tag sequence during purification and to contribute to antimicrobial activity of the mixture after the cleavage of the precursor would be particularly useful. Histidine rich antimicrobial peptides could fulfill this double role acting as tag sequences for the Immobilized Metal Affinity Chromatography (IMAC). Interesting candidates are histatins (zinc/copper binding antimicrobial peptides) and fragments of His-rich glycoprotein (His-GP). This large protein, present in the plasma of all vertebrates, contains an unstructured domain rich in histidines. For example, human His-GP contains several tandem repeats of the sequence HXHXH. It has been demonstrated that a 20 aa fragment isolated from this region has strong antimicrobial activity at acidic pH or in the presence of Zn²⁺ (obviously both conditions provide a high positive charge to the peptide) [48]. On the other hand it has been shown that sequences containing the HXH motif bind to Ni-chelate chromatographic resins even more strongly than the conventional His6 tag. This suggests that modules derived from His-GP could also act as an efficient His-tag for the purification of the modular artificial precursors.

On the basis of the considerations reported above the first synthetic precursor, herein called **AT5H**, was designed:

MKQDP-(FibA-DP-GKY20-DP)₅-HRP

Where HRP is a 22 residues region from human His-rich glycoprotein (22 aa; HPHGHHPHGHHPHGHHPHGHHP).

It should be noted that the five residues MKQDP were added at the N-terminus for two different reasons:

1) it has been demonstrated that two or more A and C rich codons following ATG codon co-operate with ribosomal binding site to increase the efficiency of translation thus providing high expression levels. As Lys and Gln are coded by the codons AAA and CAA, respectively, the addition of the KQ dipeptide provides a way to insert an A/C rich sequence after the ATG start codon;

2) as acid hydrolysis cleaves the bond between Asp and Pro internal FibA modules are released with an additional proline residue at the N-terminus. Without the sequence KQDP upstream the first FibA module, this module would be released in the form Met-FibA thus providing an heterogeneous mixture of FibA-type peptides.

All the DP sequences in AT5H have a flexible sequence, rich in small and/or coil-preferring amino acids that could provide an efficient cleavage, at least on one side as shown below:



It should be noted that the complete acidic hydrolysis of AT5H should provide a mixture of four peptides:

1. The tetrapeptide MKQD, deriving from the N-terminus.
2. The HRP peptide with an additional proline at the N-terminus [herein called (P)HRP].
3. The FibA peptide with an additional proline at the N-terminus and an additional aspartate at the C-terminus [herein called (P)FibA(D)]
4. The GKY20 peptide with an additional proline at the N-terminus and an additional aspartate at the C-terminus, herein called (P)GKY21 as an aspartate residue is naturally present in the human thrombin sequence and it has already been demonstrated that its presence or absence does not influence the antimicrobial activity of the thrombin derived AMP (i.e. GKY20 and GKY21 have the same antimicrobial activity).

The four peptide should be releases in the following molar ratios:



The synthetic gene coding for AT5H was designed with the assistance of the custom synthesis service of GenScript. Usually during the design of a synthetic coding sequence, the codon usage of the sequence is adapted to that of the host

organism to obtain high expression levels. However, in the case of the sequence coding for AT5H, the use of the optimal codon usage in each of the five units would imply the presence of five identical direct repeats. These repeats would not only make particularly difficult the preparation of the synthetic DNA but could negatively influence replication, transcription and translation. Therefore, a proprietary software developed by GenScript which allows to minimize direct and inverted repeats exploiting the degeneration of the genetic code was used (Fig. 3.12). Obviously this made not possible to fully comply with the codon usage of *E. coli*.

```

atgaaacaagaccggctgatagcggcgaaggcgacttttctggctgaaggcggcggcgtg
M K Q D P A D S G E G D F L A E G G G V
cgtgatccgggcaaatacggcttttatacgcgatgtgttcgtctgaaaaaatggattcag
R D P G K Y G F Y T H V F R L K K W I Q
aaagttatcgatccggcggacagcggcgagggtgatttctggcagaaggcgggtggcgtt
K V I D P A D S G E G D F L A E G G G V
cgtgacccgggcaaataatggtttttacacccacgtcttccgcctgaaaaaatggattcaa
R D P G K Y G F Y T H V F R L K K W I Q
aaagtatcgatccggcagactctggcgagggtgatttctggctgaagggtggcggtgtc
K V I D P A D S G E G D F L A E G G G V
cgcgatccgggtaataacggtttttacacgcgatgttttctgcctgaaaaaatggatccag
R D P G K Y G F Y T H V F R L K K W I Q
aaagtcacatcgatccggcggacagtgggtgagggcgatttctggccgaaggcgggtggcgtg
K V I D P A D S G E G D F L A E G G G V
cgcgatccgggtaaatatggcttttacacccacgtgttccgtctgaaaaaatggatccaa
R D P G K Y G F Y T H V F R L K K W I Q
aaagttatcgatccggcagattctgggtgagggcgatttctggccgaagggtggcggtgtt
K V I D P A D S G E G D F L A E G G G V
cgtgatccgggtaaatatggtttctacacgcgatgttttccgtctgaaaaaatggatacag
R D P G K Y G F Y T H V F R L K K W I Q
aaagtgatcgatccgcacgggtcatcatccgcacgggtcatcatccgcacgggtcatcatccgcacgggtcat
K V I D P H P H G H H P H G H H P H G H
catccgcacgggtcatcatccgtaa
H P H G H H P -

```

Figure 3.12. Genetic code of AT5H.

3.5 Expression and purification of AT5H

Recombinant AT5H was expressed in *E. coli* BL21DE3 strain with a yield of about 15 mg/L in Terrific Broth (TB) rich medium (Fig. 3.13). After cell lysis, AT5H was found in the insoluble fraction, as expected. However, when this fraction was washed with 0.1M Tris-HCl, pH 7.4, buffer containing 2% TritonX-100, 2 M urea, and 10 mM EDTA, a routine treatment for cleaning of inclusion bodies of Onconase-CAMP fusion proteins, AT5H was recovered into the soluble fraction. This suggests that recombinant AT5H protein forms aggregates that are not true inclusion bodies or that AT5H inclusion bodies are less stable than those formed by onconase. After dialysis in different buffers, AT5H, differently from ONC derived carriers, was soluble at both pH values 3 and 7. In both case also the majority of *E. coli* contaminant proteins remained soluble.

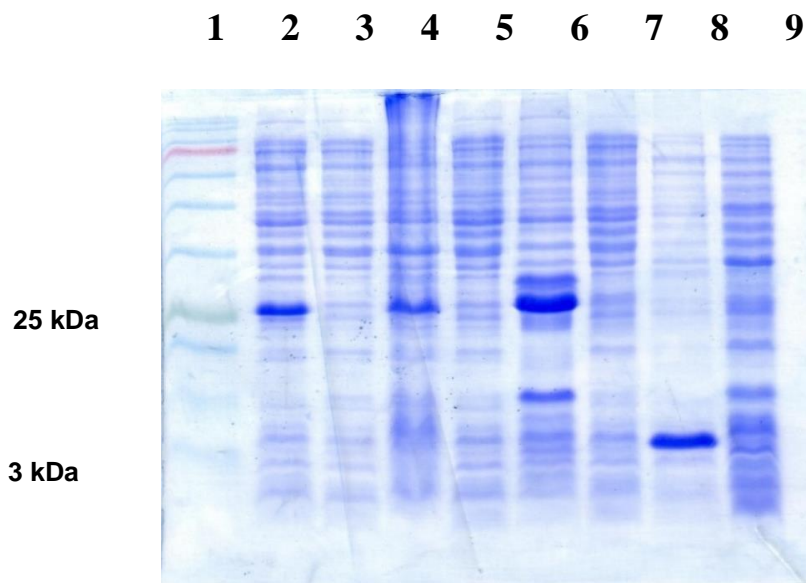


Figure 3.13: SDS-PAGE analysis of cultures expressing AT5H, AT4LH and ONC-AT2H. Analysis was performed on a 15% acrylamide gel. Lane 1: marker ladder; Lane 2: cell lysate of induced culture of AT5H 0.126 O.D; Lane 3: cell lysate of not induced culture of AT5H 0.126 O.D; Lane 4: cell lysate of induced culture of AT4LH 0.126 O.D; Lane 5: cell lysate of not induced culture of AT4LH 0.126 O.D; Lane 6: cell lysate of induced culture of ONC-DCless-H6- AT2H 0.126 O.D; Lane 7: cell lysate of not induced culture of ONC-DCless-H6- AT2H 0.126 O.D; Lane 8: cell lysate of induced culture of ONC-DCless-H6-(P)GKY20 0.126 O.D; Lane 9: cell lysate of not induced culture of ONC-DCless-H6-(P)GKY20 0.126 O.D.

Molecular weights of the protein in the marker ladder were: 245 kDa, 180 kDa, 135 kDa, 100 kDa, 75 kDa, 63 kDa, 48 kDa, 35 kDa, 25 kDa, 20 kDa, 17 kDa, 11 kDa.

As an alternative strategy for the purification the aggregates of AT5H were dissolved in guanidine-HCl denaturing buffer (pH 7.4) and loaded the solubilized material on a Ni-sepharose column. As expected, due to the presence of the HRP module, AT5H showed a good affinity for the Ni-sepharose phase. After elution about 95% of the total fusion protein with more than 95% purity. (Fig. 3.14) was recovered.

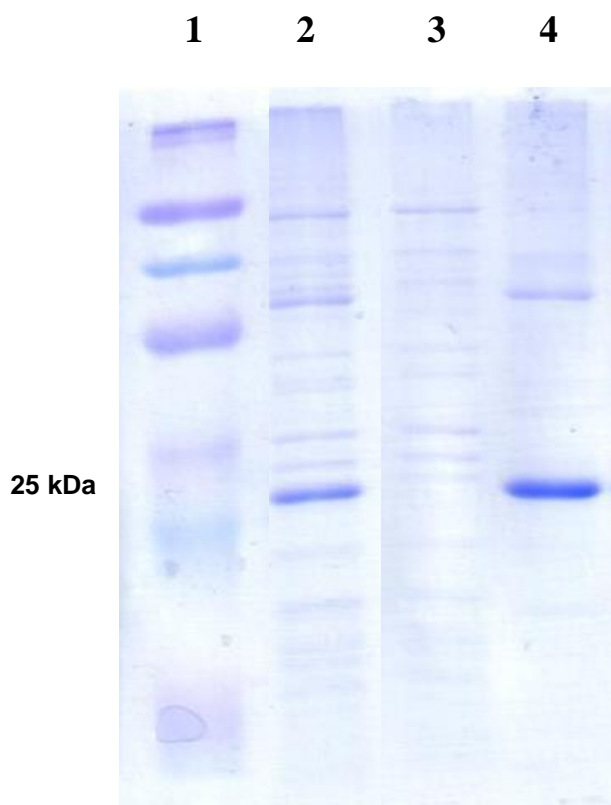


Figure 3.14. SDS-PAGE (15%) analysis of fusion proteins.

Lane 1: Ladder marker; lane 2: insoluble fractions before IMAC purification; lane 3: flow through of IMAC; lane 4: purified fusion protein by IMAC.

Molecular weights of the protein in the marker ladder were: 180 kDa, 135 kDa, 100 kDa, 75 kDa, 63 kDa, 48 kDa, 25 kDa, 20 kDa, 17 kDa, 11 kDa.

Purified AT5H recombinant protein was then dialyzed against 0.1 M acetic acid and hydrolyzed at 60 °C, pH 2 for 24 h. SDS-PAGE analyses of the cleavage product indicated that chemical cleavage occurred with very high efficiency. In fact, no band was observed at the molecular weight expected for the unhydrolyzed protein. Moreover, about 80% of the hydrolyzed fragments were observed at the position expected for peptides ~20-residues long, whereas less than 20% of the hydrolyzed fragments were observed at the position expected for ~40-residues long peptides [likely a mixture of (P)FibA-DP-GKY21, (P)GKY20-DP-FibA and/or (P)GKY20-DP-HRP modules]. No other band was observed thus indicating an almost complete hydrolysis of all Asp-Pro sites (Fig. 3.15).

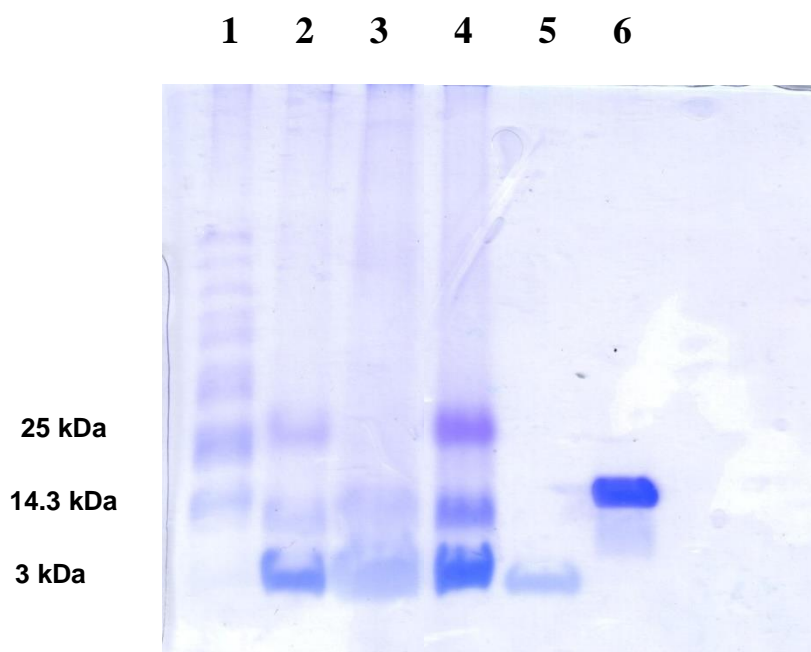


Figure 3.15. Lane1: purified fusion protein by IMAC; lane 2: acid cleavage pattern; lane 3: insoluble fraction after neutralization at pH 7; lane 4: soluble fraction after neutralization at pH 7; lane 5: ONC-DCless-H6-(P)GKY20; lane 6: ONC-DCless-H6-(P)PAP-A3 fusion protein. Gels (20 %) were stained by Coomassie Brilliant Blue R-250 in the presence of 4% formaldehyde.

3.7 Expression and purification of AT4LH

The recombinant protein AT4LH was purified following the purification procedure already used for AT5H.

AT4LH was expressed in *E. coli* BL21DE3 strain with a yield of about 30 mg/L, hence only slightly higher than AT5H. After cell lysis, AT4LH was found in the insoluble fraction, as expected. However, when this fraction was washed with 0.1M Tris-HCl, pH 7.4 buffer containing 2% TritonX-100, 2 M urea, and 10 mM EDTA, AT4LH was identified into the soluble fraction together with several *E. coli* proteins as previously observed for AT5H. In order to find an alternative washing buffer, AT4LH inclusion bodies were divided into two aliquots which were washed in denaturing buffer (pH 7.4) containing guanidine-HCl at final concentrations of 0.5 and 1 M for 20h at room temperature. SDS-PAGE analyses showed that the buffers containing 0.5 M and 1M guanidine-HCl allowed to remove 10% and 40% of the contaminant *E. coli* proteins, respectively, without solubilizing AT4LH. The pellet obtained by centrifuging the inclusion bodies washed with the buffer containing 1 M guanidine-HCl were further washed with a buffer containing 1.5 M of guanidine-HCl. In this case SDS-PAGE analyses showed that 98% of the AT4LH was in the soluble fraction whereas the insoluble fraction contained essentially *E. coli* proteins. The solubilized AT4LH was further purified by immobilized metal ion affinity chromatography (IMAC). About 95% of AT4LH with more than 85% purity was recovered.

Purified AT4LH recombinant protein was then dialyzed against 0.1 M acetic acid and hydrolyzed at 60 °C, pH 2 for 24 h. SDS-PAGE analyses of the hydrolyzate showed that AT4LH gives a fragmentation pattern essentially identical to that obtained in the case of AT5H (fig. 3.16). Final yield of the peptide mixture was about 6-7 mg/L of culture.

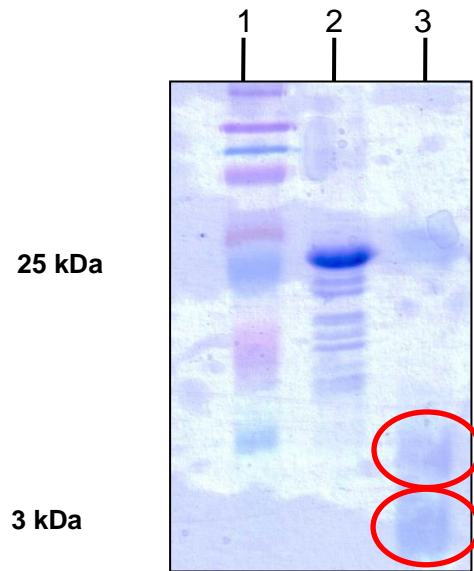


Figure 3.16: SDS-PAGE analysis of AT4LH hydrolysis products. Analysis was performed on a 20% acrylamide gel. Lane 1: marker ladder; Lane 2: purified fusion protein AT4LH in acetic acid 0.1M; Lane 3: Acid cleavage of AT4LH; Molecular weights of the protein in the marker ladder were: 180 kDa, 135 kDa, 100 kDa, 75 kDa, 63 kDa, 48 kDa, 25 kDa, 20 kDa, 17 kDa, 11 kDa.

3.8 Cloning, expression and purification of **ONC-AT2H**

As also the carrier-less modular protein AT4LH provided unsatisfactory expression levels we decided to create a fusion protein between the carrier ONC-DCless-H6 and the C-terminal half of the modular protein AT4LH. By cloning the BamHI/SacI fragment present at the 3' of the ORF coding for AT4LH, described in section 3.6, into the vector pET22/ONC-DCless-H6 already available in our laboratory we prepared the expression vector named pET22/ONC-AT2H allowing the expression of the fusion protein **ONC-AT2H**:

ONC-DCless-H6-DP-(FibA-DP-GKY20-DP)₂-HRP

It should be noted that five AMP modules are appended to the C-terminus of the ONC derived carrier and that the modular part has a length comparable to that of the carrier (103 and 120 residues respectively).

The complete acidic hydrolysis of ONC-AT2H should provide a mixture of four peptides in the following molar ratios:

$$\text{ONC-DCless-H6} : (\text{P})\text{HRP} : (\text{P})\text{FibA(D)} : (\text{P})\text{GKY21} = 1 : 1 : 2 : 2$$

Recombinant ONC-DP-AT2H was expressed in *E. coli* BL21DE3 strain with a yield of about 120 mg/L in Terrific Broth (TB) rich medium (Fig. 3.17a). After cell lysis, ONC-AT2H was found in the insoluble fraction, as expected (Fig. 3.17b). When this fraction was washed with 0.1 M Tris-HCl, pH 7.4 buffer containing 2% TritonX-100, 2 M urea, and 10 mM EDTA, a routine treatment for cleaning inclusion bodies of onconase-CAMP fusion proteins, ONC-AT2H was found into the insoluble fraction thus confirming that an ONC module is necessary to obtain high insoluble inclusion bodies.

By IMAC purification a recovery of about 95% of the total fusion protein with more than 95% purity was achieved. Purified ONC-AT2H was then dialyzed against 0.1 M acetic acid and hydrolyzed at 60 °C, pH 2 for 24 h. SDS-PAGE analyses (Fig. 3.18) of the cleavage product indicated that cleavage occurred at a very high efficiency: about 80% of the recombinant protein was cleaved to the expected peptides ~20-residues long. In order to remove the onconase from the sample, a selective precipitation was performed by adjusting pH at 7.2 by addition of ammonia. About 15-16 mg of the peptide mixture were obtained. HPLC and mass analysis allowed to confirm that the main products of the acid cleavage are the expected peptides (P-ThrAP-D; P-FibA-D and P-HRP) and the ONC-D protein (Fig. 3.19 and Table 2).

Comparing the results obtained from the two modular proteins, AT4LH and ONC-DP-AT2H, it can be concluded that ONC-DP-AT2H provides higher yields with a simpler purification procedure.

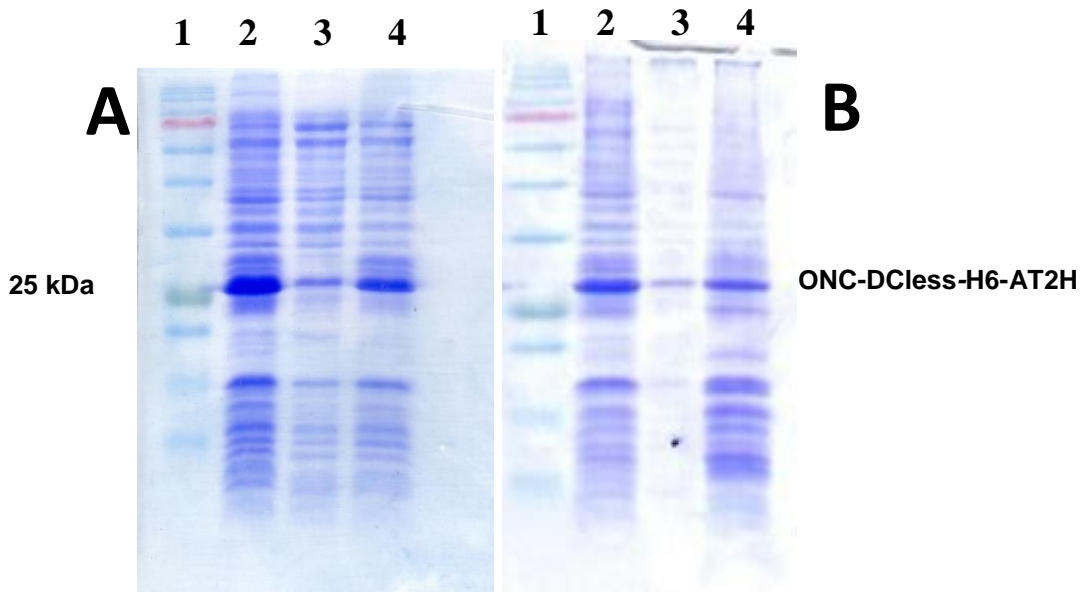


Figure 3.17: Purification of peptides mixture. 15% SDS analysis.(A) Lane 1: marker ladder; Lane 2: cell lysate of induced culture of ONC-DCless-H6- AT2H 0.126 O.D; Lane 3: cell lysate of analytical not induced culture of ONC-DCless-H6- AT2H 0.126 O.D; Lane 4: cell lysate of analytical induced culture of ONC-DCless-H6- AT2H 0.126 O.D. (B) Lane 1: marker ladder; Lane 2: cell lysate of induced culture of ONC-DCless-H6- AT2H; Lane 3: cell lysate of soluble fraction of ONC-DCless-H6- AT2H; Lane 4: cell lysate of insoluble fraction of ONC-DCless-H6- AT2H. Molecular weights of the protein in the marker ladder were: 245 kDa, 180 kDa, 135 kDa, 100 kDa, 75 kDa, 63 kDa, 48 kDa, 35 kDa, 25 kDa, 20 kDa, 17 kDa, 11 kDa.

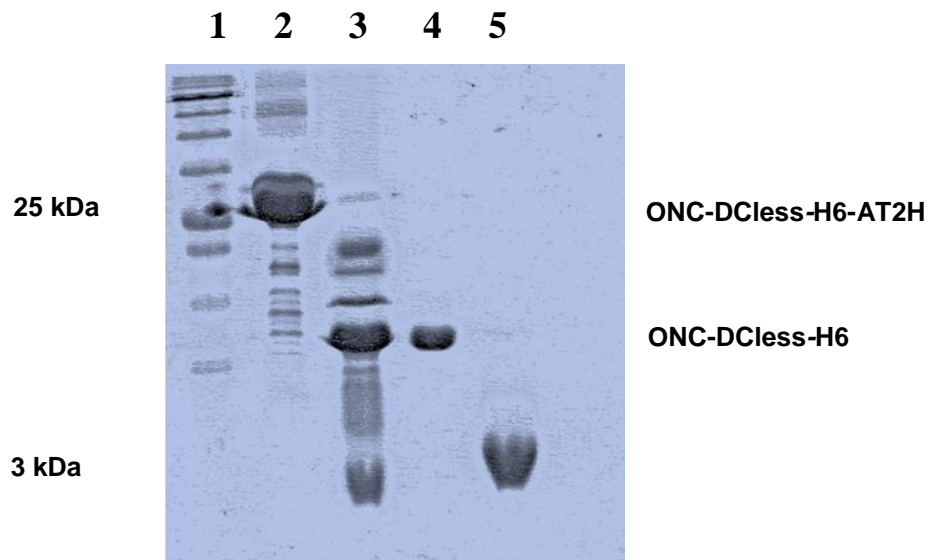


Figure 3.18: SDS-PAGE analysis of ONC-AT2H. Analysis was performed on a 20% acrylamide gel. Lane 1: marker ladder; Lane 2: purified ONC-AT2H in acetic acid 0.1M; Lane 3: Acid cleavage of ONC-AT2H; Lane 4: Insoluble fraction after neutralization at pH 7; Lane 5: Soluble fraction after neutralization at pH 7. Molecular weights of the protein in the marker ladder were: 245 kDa, 180 kDa, 135 kDa, 100 kDa, 75 kDa, 63 kDa, 48 kDa, 35 kDa, 25 kDa, 20 kDa, 17 kDa, 11 kDa.

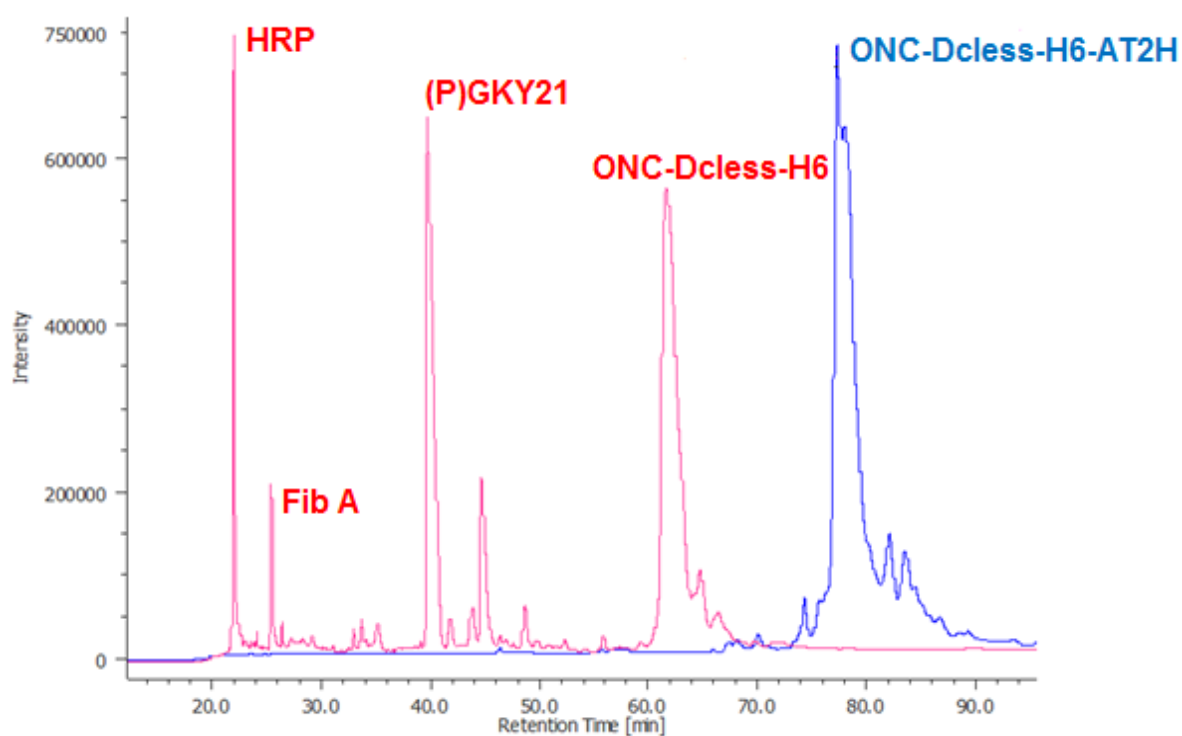


Figure 3.19: RP-HPLC analysis of hydrolyzed ONC-AT2H.

Blue line, purified ONC-AT2H; pink line hydrolyzed ONC-AT2H. Absorbance was recorded at 230 nm.

Peak	Experimental weight ($[M+H]^+$)	Theoretical weight ($[M+H]^+$)	Sequence position
Peak 1	2611.19 ^a	2612.76	195-217 (HRP)
Peak 2	1748.75 ^a	1749.78	115-132/155-172 (FIBA)
Peak 3	2723.46 ^a	2724.25	133-154/173-194(GKY21)
Peak 4	13364 ^b	13363	1-114 (ONC-DCless-H6)
Peak 5	24848 ^{b,c}	24831	1-217(ONC-DCless-H6-AT2H)

^a TOF reflectron mode.

^b TOF linear mode.

^c The observed difference between the theoretical and the experimental molecular weight (17 Da) may be caused by the oxidation of residue Met(-1) in the fusion protein. This oxidation has been observed in other fusion proteins containing ONC-DCless-H6 as a carrier.

Table 2: Mass spectrometry analysis.

In the table shows the theoretical and experimental weight of the peaks obtained by HPLC and analyzed by mass spectrometry.

3.9 Antimicrobial activity of AT2H

In order to study the antimicrobial activity of the peptide mixture derived from the hydrolysis of ONC-AT2H, dose-effect curves were carried using (P)GKY20 as positive control. The activity of (P)GKY21 purified from the mixture by HPLC was also assayed.

The comparison of the activities of a single AMP and a mixture of three AMPs is not trivial. As the mixture contains (P)GKY21 (which corresponds to 2/5 of the mixture on a molar basis) the concentration of the mixture was expressed as “molar equivalents” of peptide (P)GKY21. Thus, for example, 1 μM of mixture corresponds to 1 μM of (P)GKY21, 1 μM of (P)FibA(D) and 0.5 μM of (P)HRP.

As shown by the curves in Fig. 3.20, (P)GKY20 and (P)GKY21 show essentially the same activity as expected from the literature data, whereas, the mixture containing also (P)FibA(D) and (P)HRP is considerably more active thus suggesting that these two AMPs contribute significantly to the antimicrobial activity of the mixture. At the moment it is not possible to determine the relative contribution of (P)FibA(D) and (P)HRP and if the activity of these peptide is additive or synergic with that of (P)GKY21. The answers to these questions will first require the purification of adequate quantities of (P)FibA(D) and (P)HRP.

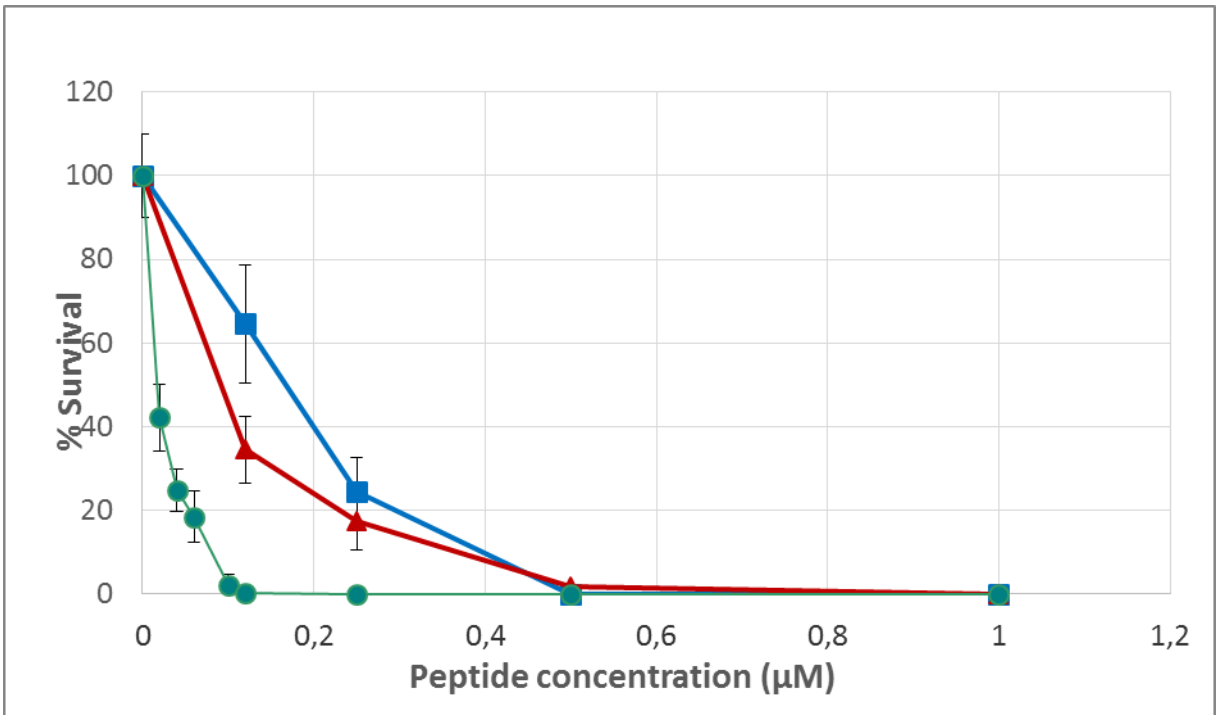


Figure 3.20: Viable count assay of the peptide mixture from ONC-AT2H.

Blue squares, GKY20; red triangles, GKY21; green circles, peptide mixture obtained by hydrolyzing ONC-AT2H.

Chapter 4-Conclusions

The activities of the present PhD thesis have been carried out in the context of a wide research project whose main goal is the development of human AMPs-based antimicrobial drugs for topic applications like treatment of surgical wounds, ulcers and skin, mouth and airways infections. The main aim of the project is the development of strategies and tools for the production of AMPs and in particular of production strategies allowing an easy scale up from the laboratory scale to the pilot and even the industrial scale. In this context our research group has already developed an optimized carrier (ONC-DCless-H6) for the production of recombinant AMPs as fusion proteins in *E. coli*. This method not only provides high amount of peptides with high purity but also involves relatively few purification steps, thus allowing to limit production costs. The specific aim of the present project is to further widen the applicability of our approach to the production of mixtures of two or more AMPs. The pharmacological potential of such mixtures is high but the cost and the complexity of production has discouraged, until now, their development. Therefore, a strategy to prepare mixtures of two or more AMPs with costs, production times and amount of work comparable to those necessary for the production of a single recombinant AMP would open the way to the exploitation of AMP mixtures.

Two alternative strategies were evaluated, one still exploiting the previously optimized onconase-based carrier and an alternative strategy aiming to prepare carrier-less precursors composed only by AMP modules thus minimizing the production of “waste material”.

The characterization of the proteins ONC-DCless-H6-(P)PAP-A3(Pro26) and ONC-DCless-H6-AT2H has confirmed the excellent performances and the reliability of the carrier based method. ONC-DCless-H6 was able to effectively drive to inclusion bodies both a highly cationic sequence of about 50 residues containing two CAMP-like sequences [(P)PAP-A3(Pro26)] and a modular sequence of more than 100 residues including anionic, cationic and histidine rich modules (AT2H). In both cases the expression yields were high (>200 mg/L and >100 mg/L, respectively) and the purification by IMAC provided a protein with good yield and purity.

As for the cleavage at the multiple junction sites, a crucial point of any strategy for the production of multiple peptides from a single precursor, acid cleavage in 0.1 M acetic acid at 60°C confirmed to be a reliable, easy and “green” strategy (not including organic solvents, toxic reagents or harsh condition). The efficiency was very high in the case ONC-DCless-H6-AT2H which essentially provided only the desired peptides, thus indicating that all the acid labile Asp-Pro sequences underwent cleavage with an efficiency likely higher than 95% (indeed incomplete cleavage products were not distinguishable from the background of the RP-HPLC chromatogram). After the acidic cleavage, the mixture was easily separated from the carrier by simply changing the pH to cause the aggregation of the carrier. The mixture of peptides which was obtained by our procedure contained only the desired peptides, and was used in biological assays to test their efficiency as antimicrobial agents without any further purification. In the perspective of a scale up of the production this is obviously a particularly advantageous feature. On the contrary, in the case of ONC-DCless-H6-(P)PAP-A3(Pro26), the internal Asp-Pro sequence was cleaved with an efficiency of only about 85%. Thus, after precipitation of the carrier, the mixture contained a significant amount (about 10% by weight) of the not-cleaved (P)PAP-A3(Pro26) peptide. The comparison of the sequences adjacent to the different Asp-Pro cleavage sites in ONC-DCless-H6-

(P)PAP-A3(Pro26) and ONC-DCless-H6-AT2H suggested that in order to obtain a very high cleavage efficiency a flexible sequence, rich in small and/or coil-preferring amino acids, should be present at least on one side of the Asp-Pro site. This information will be useful for the design of further fusion proteins.

In the case of the carrier-less modular precursors the results were less positive but, nonetheless, they provided useful indications for a future optimization of this alternative strategy. Both modular proteins AT5H and AT4LH showed relatively low expression levels (15 and 30 mg/L, respectively) and the formation of inclusion bodies which, differently from those generated by ONC-DCless-H6, were soluble in 2 M urea suggesting a lower compactness/stability. Possible causes of the low expression levels could be the non-optimal codon usage necessary to avoid the presence of 4-5 identical direct repeats in the coding sequences. The low expression levels, in turn, could contribute to the formation of the “unstable” inclusion bodies. Indeed, it is well known that inclusion bodies formation is generally related to high expression levels. It should be noted that alternatives to the direct chemical synthesis of repetitive DNA sequences are well described in literature. For example small DNA fragments can be joined by ligation to produce long sequences with variable number of identical direct repeats. In the future this kind of approach could allow preparing coding sequences where all the repeats have an optimal codon usage.

In conclusion we believe that, even if not all the initial objectives have been fully achieved, this PhD work will pave the way to the development of pharmacologically interesting peptide mixtures.

Chapter 5-Period Abroad

5.1 *Myxococcus xanthus*

Myxococcus xanthus is a soil bacterium which commonly grows in damp soil rich in organic matter (Fig. 5.1). The bacteria are rod shaped and 10 times bigger than *E. coli* in size, able to use peptides, lipids and other macromolecules for nutrition and tend to form large multicellular communities, which feed upon other microorganism, utilizing extracellular antibiotics and degradative enzyme to immobilize and digest their prey [52-53-54].

M. xanthus is one of many diverse Gram-negative bacteria which move by gliding motility. Gliding motility is generally described as the movement in the direction of the long axis of the cell at a solid-liquid, solid-air or air-liquid interface without the aid of flagella [55]. *M. xanthus* has two genetically distinct systems for motility.

The first system, known as social (S)-motility and involves the movement of cells in group [56]. The second one, known as adventurous (A)-motility and involves the movement of single cells.

S-motility requires type IV pili, lipopolysaccharide (LPS) O-antigen, and extracellular matrix polysaccharide (called fibrils). Type IV pili are particularly determinant for S-motility: it has been shown indeed that pili, extruded from one cell pole, adhere to the exopolysaccharide deposited on a surface or on another cell so that following retraction of the pilus, pulls the cell in the direction of the site of adhesion [57-58-59-60].

A- motility is not yet clarified so far. A commonly accepted hypothesis assumes the extrusion of a polyelectrolyte gel to push the cell forward [61]. A more recent model proposes that intracellular motor complexes, connected to both membrane-spanning adhesion complexes and to the cytoskeleton, enhance the motility by pushing cell body towards to the substratum, in a way similar to focal adhesion-based traction or apicomplexan gliding motility in eukaryotic organisms [62].

M. xanthus cells periodically reverse their direction of movement and cell reversals are thought to be required for directional adjustment as part of the biased random walk necessary for chemotaxis. In nature, when *M. xanthus* swarming cells are unable to find sufficient nutrients, they enter a developmental process in which they aggregate forming raised pigmented mounds, termed fruiting bodies. Cells encapsulated inside fruiting bodies differentiate to form spores. Spores are metabolically dormant cells that can withstand prolonged periods of starvation, desiccation, and relatively high temperatures for their soil habitat. The process of sporulation involves the rounding up of the cells and the restructuring of the cell wall [53-54]. Although fruiting bodies involve the majority of cells (80-90%) aggregate to form fruiting bodies, some cells may follow a different developmental fate. It has been hypothesized that they could be scout cells, since spores cannot search for prey [63].

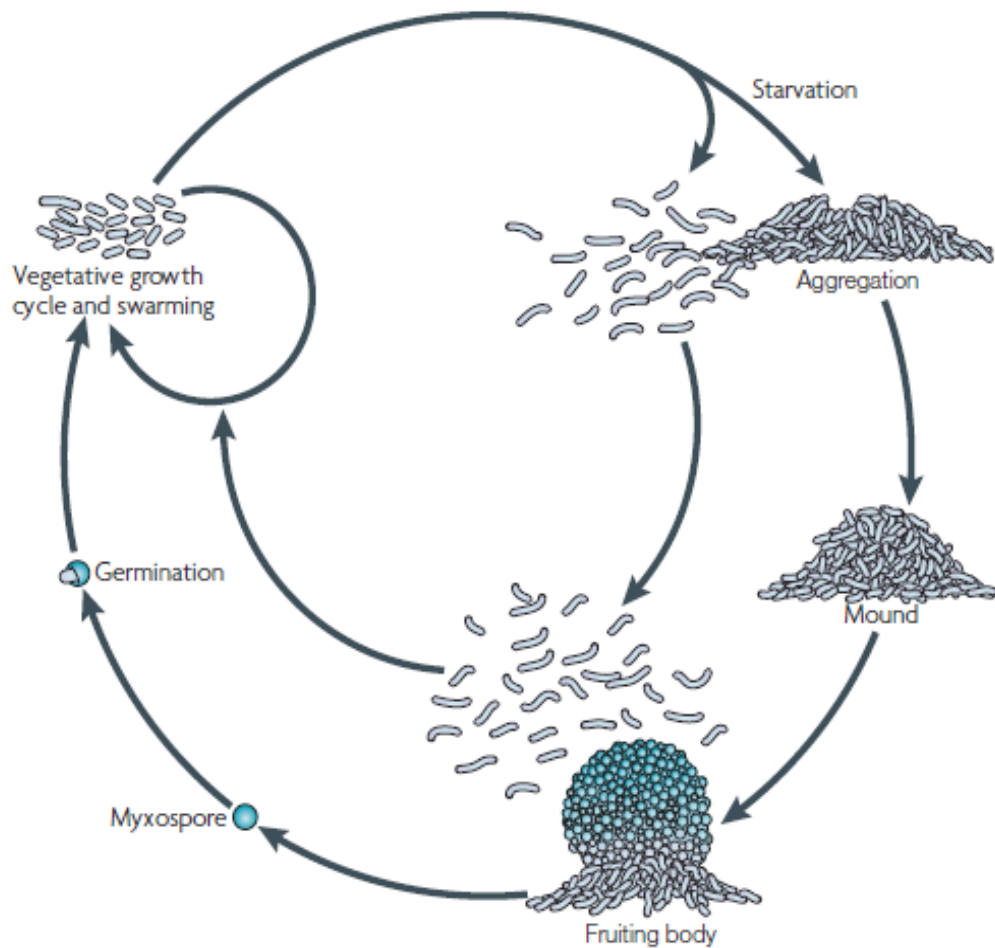


Figure 5.1: Life cycle of *Myxococcus xanthus*.

Myxococcus xanthus cells are usually found on solid substrates. When nutrients are present, groups of cells (swarms) grow and divide and move outward in search of additional macromolecules or prey. Upon starvation, cells aggregate at discrete foci to form mounds and then macroscopic fruiting bodies. The rod-shaped cells in the fruiting bodies undergo morphogenesis and form spherical spores that are metabolically inactive and partly resistant to desiccation and temperature. Peripheral rods remain outside fruiting bodies and move as accordion waves in their search for food. When nutrients become available, the spores germinate and complete the life cycle. [64]

5.2 Frz system

The Frz chemosensory system controls directed motility in *M. xanthus* by regulating cellular reversal frequency. In contrast to *E. coli*, *M. xanthus* has eight chemotaxis-like pathways [65], four of which have been characterized [66-67-68-69].

The Frz system was the first pathway to be studied and is responsible for controlling the frequency at which individual cells reverse their direction of movement (Fig. 5.2) [70-71-72]. *M. xanthus* requires the Frz system for vegetative swarming on rich media and for cellular aggregation during fruiting body formation on starvation media. In fact, directional control is required for cells to move in a biased random walk during colony swarming and for aggregation during fruiting body formation. The Frz system consists of: FrzCD, a cytoplasmic chemoreceptor; FrzA and FrzB, two CheW-like proteins (CheW domain is topologically similar to SH3 domains from eukaryotic scaffold proteins that also play a role in signal transduction [73-74]); FrzE, a CheA–CheY fusion protein; FrzF, a methyltransferase; FrzG, a methylesterase; and FrzZ, a CheY–CheY fusion protein [66-75]. These proteins share homology with chemotaxis proteins from enteric bacteria, which are encoded in the *frzA-F* operon and the divergently transcribed *frzZ* gene.

Mutants containing transposon or plasmid insertions in the *frz* genes rarely reverse their direction of gliding and are defective in swarming [72]. Furthermore, *frz* mutants are unable to form fruiting bodies when starved but at the contrary tend to aggregate into tangled filaments evolving in a phenotype termed 'frizzy' [70-72-76]. FrzCD, the Frz chemoreceptor, contains a conserved C-terminal module present in methyl-accepting chemotaxis proteins (MCPs); but, in contrast to most MCPs, FrzCD is localized in the cytoplasm and the N-terminal region of FrzCD does not contain transmembrane or sensing domains, or even a linker region.

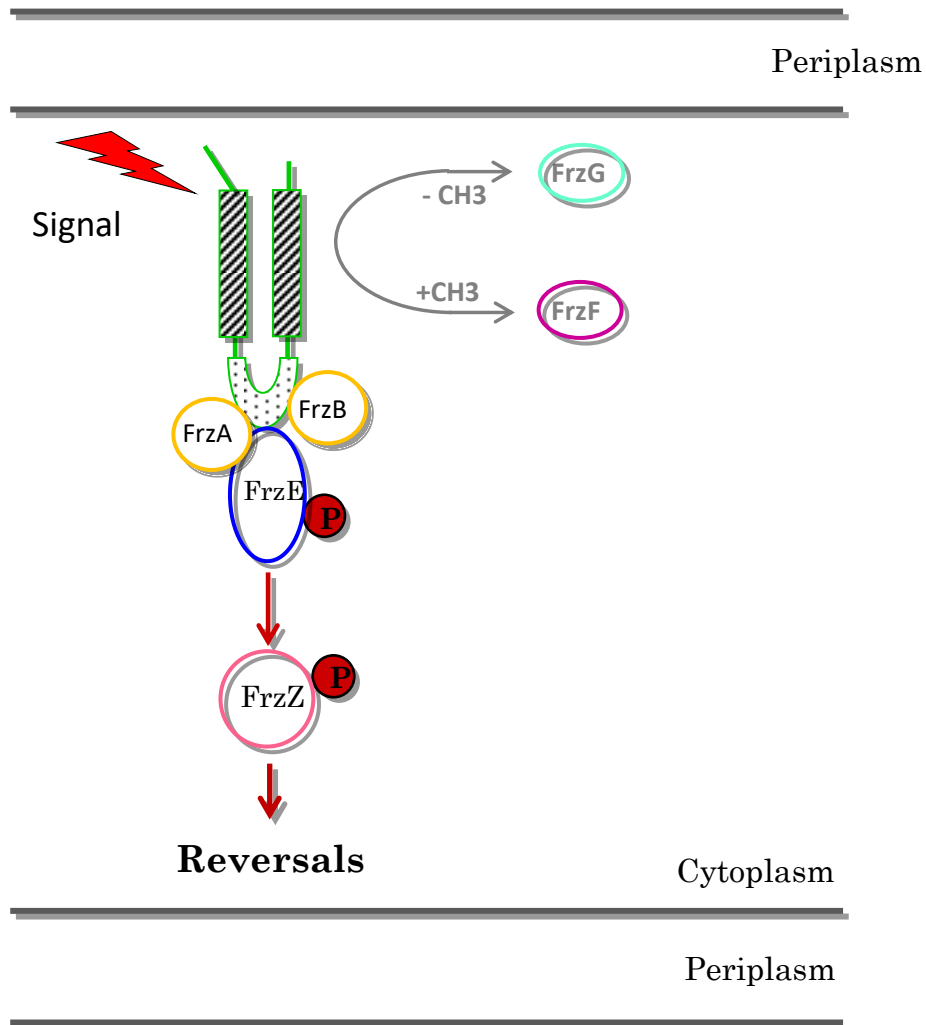


Figure 5.2: The Frz system.

The Frz system consists of: FrzCD, a cytoplasmic chemoreceptor; FrzA and FrzB, two CheW-like proteins; FrzE, a CheA–CheY fusion protein; FrzF, a methyltransferase; FrzG, a methylesterase; and FrzZ, a CheY–CheY fusion protein [16].

5.3 Construction of a $\Delta frzA \Delta frzB frzB^{A\beta4\beta5}$ strain producing the FrzB^{A β 4 β 5} Chimera

Frz system (see Figure 5.2) has two CheW-like proteins, FrzA and FrzB. CheW-like protein are normally involved in the connection between the receptor and the kinase. We wondered why the Frz system needed two CheW. To better understand the function of FrzA and FrzB we first deleted each of the corresponding genes and looked at phenotypes.

We found that the phenotypes are different from wt (Fig. 5.3); Figure 5.3 shows that FrzA is required for all the observed phenotypes and that is, thus, the core CheW of the system. On the other hand, FrzB is not required for the response to the isoamyl alcohol, a known activator of the Frz system [69-77], which suggests that this protein might have a different role.

By aligning the protein sequences of FrzB and FrzA with that of the CheW from *Thermatoga maritime* (performed by research group of Dr. T. Mignot), we found that FrzB lacks a 20 amino acid region. To check whether this region have a function in the FrzB interaction on protein structure, the workshop where I did my time abroad, has been awarded the structural model of the FrzE^{P4-P5}:FrzA and FrzE^{P4-P5}:FrzB interactions by using the *T. maritime* CheA^{P4-P5}:CheW crystal structure as template (Fig. 5.4), we found that the 20 amino acid region present in FrzA but not in FrzB, is predicted to form a two beta sheet (β 4 and β 5) loop located at the interface with the CheA P5 domain and specifically involved in the CheW:CheA interaction [78]. Our analysis, thus, suggests that FrzB lacks the FrzE binding region.

To confirm that FrzB did not interact with its cognate histidine kinase, we performed bacterial two-hybrid assays. As expected, both FrzA and FrzB interacted with FrzCD as well as with the FrzCD signaling domain alone (FrzCD_{SD}). On the other hand, only FrzA but not FrzB interacted with the FrzE P5 domain (FrzE_{P5}). Neither FrzA nor FrzB could interact with the FrzCD N-terminal domain. These results altogether suggest that FrzB does not interact with FrzE.

We then decided to construct a recombinant strain producing in the place of both FrzA and FrzB, a chimeric protein obtaining by introducing 21 amino acids from FrzA into FrzB at positions 476-497. The resulting strain responded to IAA (Fig. 5.3), meaning that the chimera could bind the histidine kinase.

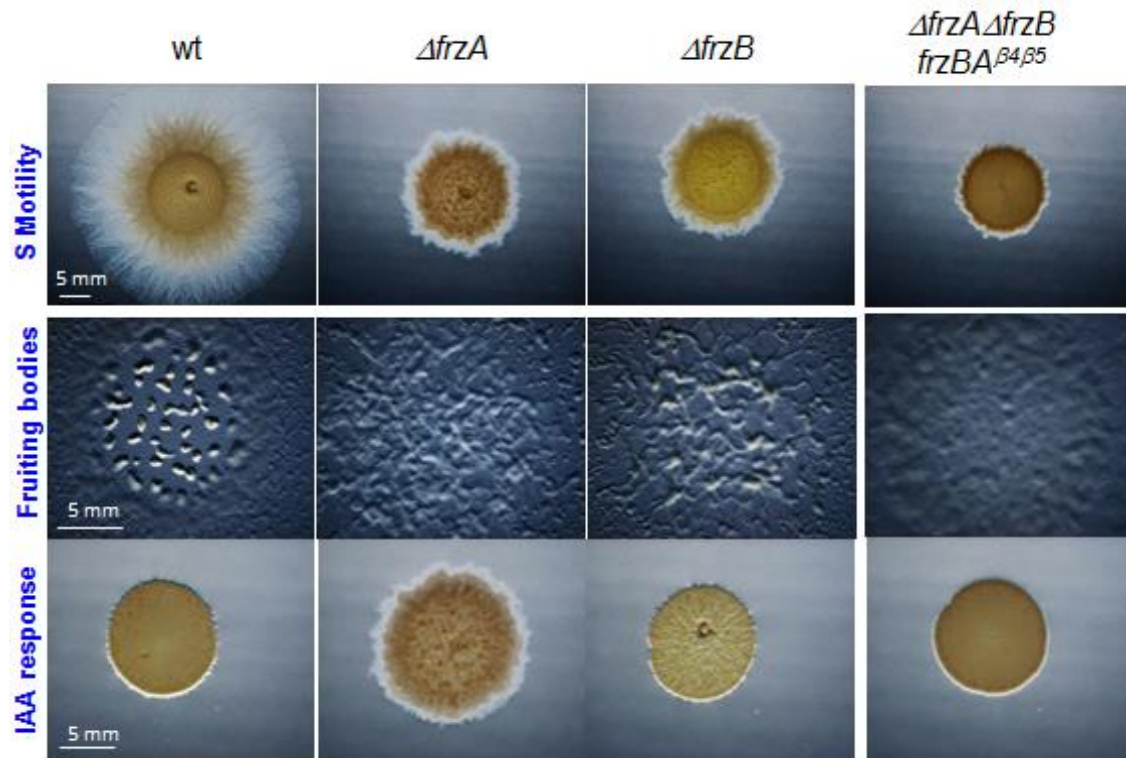


Figure 5.3: The Chimera phenotypes.

For S-motility it was used a plate with CYE agar at 0.5%; for fruiting bodies was used a plate with CF agar at 1.5%; for the IAA response was used a plate with CYE agar at 0.5% and 0.15% IAA. By phenotypes, therefore, it is clear that FrzA is the kinase of the main system and that the addition on a to beta sheets from FrzA (B4 and B5) to FrzB, allowed this protein to act as a real CheW.

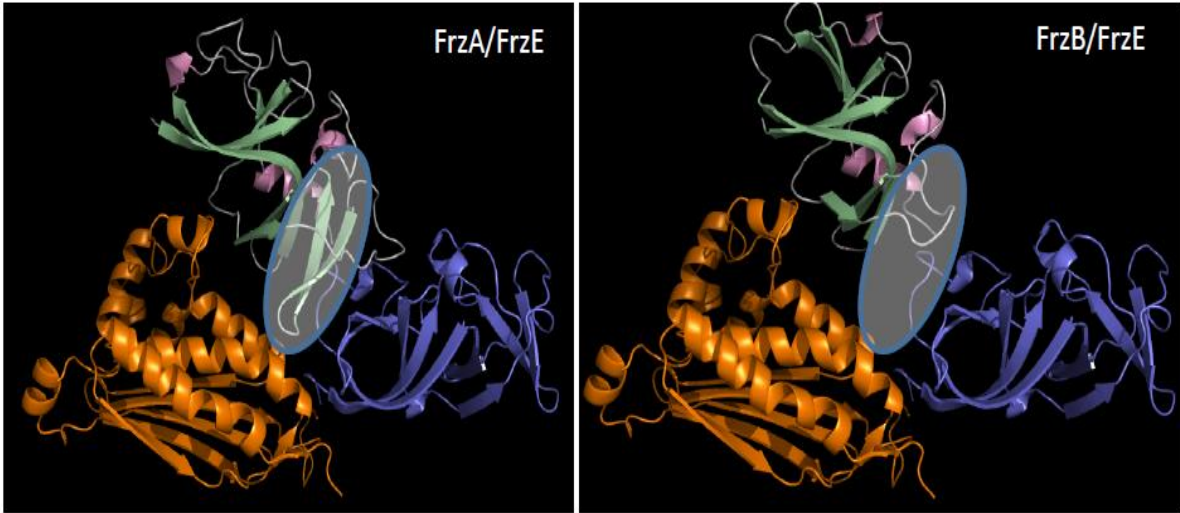


Figure 5.4: Model structure of FrzA/FrzE and FrzB/FrzE.

B lacks a part of A, composed of two beta sheets, which connects it to the kinase

5.4 Production of a FrzCD Δ 131-180mutant

Canonical receptors from *E.coli*, consist of a transmembrane domain, a ligand binding domain, a HAMP domain, and a signaling region. HAMP is a flexible region that changes when the receptors senses the signal and transfers the conformational change to the domain of methylation (shaped of hook in figure 5.5a).

Instead, the FrzCD receptor from *M. xanthus*, does not have transmembrane domains and has a HAMP domain degenerated. It is therefore a cytoplasmic receptor (figure 5.5b). This receptor binds to the bacterial nucleoid, employing it as a support to recruit all signal proteins. The region extending from aa 7-27 was identified as a positively charge peptides that has a very important role in DNA-binding [79] while the region ranging from 131 to 180 has unknown function. To understand the role that the 131-180 portion has within the genome, the deletion of this same portion was carried out, thus creating a new mutant called *frzCD Δ 131-180*. After obtaining the plasmid to construct the mutant of interest, transformation of the *M. xanthus* cells with the plasmid of interest was performed. Once carried out a screening of the colonies, we continued with the selection with the galactose to lop out the plasmid and have a clean deletion mutant.

This is because if it takes place on a single recombination, the wt gene will be reconstituted, allowing the formation of a halo around the colony. Otherwise if both recombinations occur there will be a rearrangement of genes and you will get our mutant of interest having colonies lacking of halos.

Having used a double-recombinant system, this type of selection will guarantee us that colonies not presenting a halo have had a double-recombinant system and will be therefore mutants of interest.

In our phenotype analysis (Fig. 5.6), we can see that, unlike wt, the *frzCD Δ 131-180* mutant, shows no colony expansion and no fruiting bodies. This phenotype is due to the fact that cells are hyper-reversing and cannot produce a net swarming.

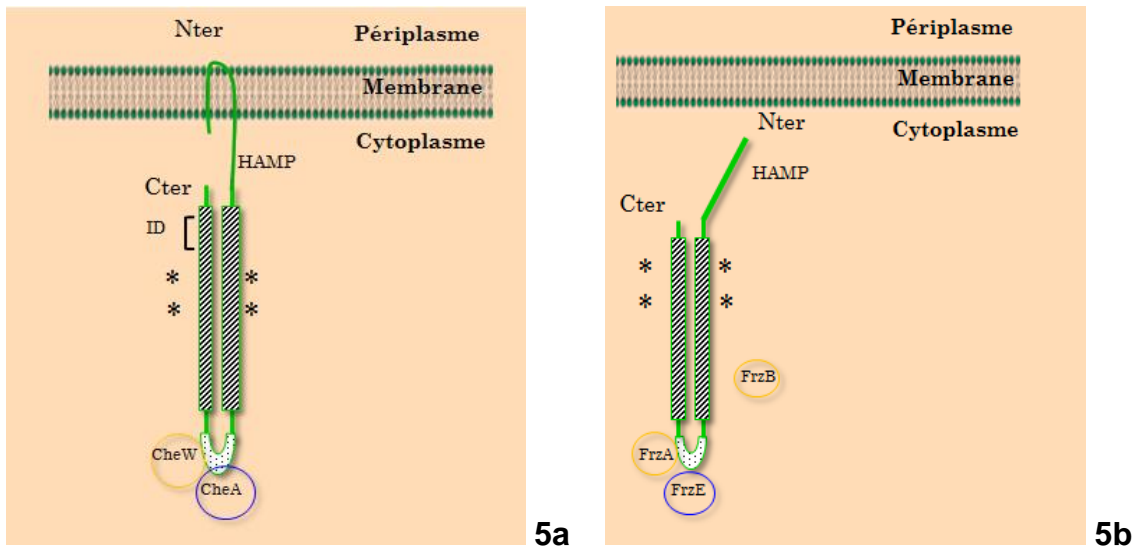


Figure 5.5: a) canonic receptor of *E.coli*; b) receptor of *M.xanthus*.

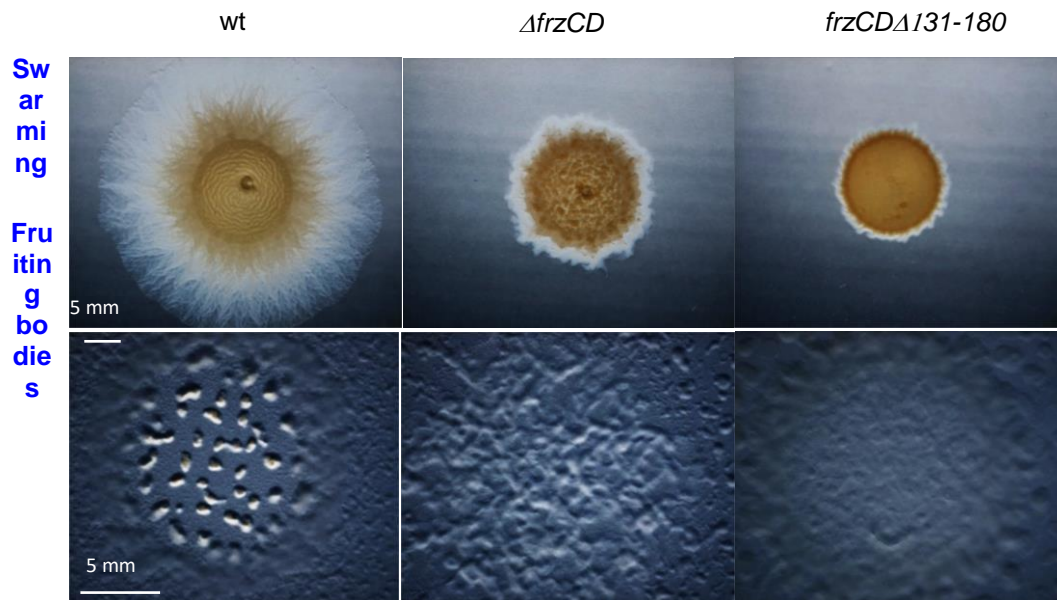


Figure 5.6: The $FrzCD\Delta 131-180$ mutant phenotypes.

For S-motility it was used a plate with CYE agar at 0.5%; for fruiting bodies was used a plate with CF agar at 1.5%;

5.5 Materials and methods

Strains used in this thesis are: *DZ2 WT*, *EM523 (Δ frzA)*, *EM524 (Δ frzB)*, *EM605 Chimera frzAB*, *EM525 (Δ frzCD)*, *frzCD Δ 6-182*, *frzCD Δ 6-130*, *frzCD Δ 131-180 #1*, *frzCD Δ 131-180 #6*.

Vectors used in this thesis are: *pETPhos* and *pBJ113*.

Plasmid used in this thesis is *pEM467*.

For sequencing, it was used the company GATC Biotech.

M. xanthus strains were grown at 32°C in CYE rich media over night. Plasmids were introduced into *M. xanthus* cells by electroporation. These strains were obtained by homologous recombination based on a previously reported method using the *pBJ113* or *pBJ114* vectors [77-80].

Escherichia coli cells were grown under standard laboratory conditions in Luria-Bertani broth supplemented with antibiotics if necessary.

For swarming assays, cells (5 μ l) at a concentration of 5×10^9 cfu ml⁻¹ were spotted on CYE agar plates and incubated at 32°C and photographed after respectively 48h with an Olympus SZ61 binocular stereoscope. For predation assays, *M. xanthus* cells (3 μ l at a concentration of 5×10^9 cfu ml⁻¹) were spotted at 0.7 mm distance from each other on CF agar plates, incubated at 32°C and photographed after 72 h.

Land used for the growth of phenotypes, are:

- S-motility: CYE agar at 0.5%;
- Fruit Bodies: CF agar at 1.5%;
- IAA response: CYE agar at 0.5% and IAA at 0.15%.

References

- [1] Zasloff, M. **Antimicrobial peptides of multicellular organisms**, 2002 Nature 415:389-95
- [2] Wiesner J. and Vilcinskas A. **Antimicrobial peptides the ancient arm of the human immune system**, 2010. Virulence 1(5):440-464.
- [3] Hancock R. E. W., Haney E. F., Gill E. E. **The immunology of host defence peptides: beyond antimicrobial activity** 2016 Nat Rev Immunol. 16:321-34.
- [4] N. Motamedi, L. Danelishvili, L.E. Bermudez **Identification of *Mycobacterium avium* genes associated with resistance to host antimicrobial peptides** J. Med. Microbiol. 2014, 63, 923–930.
- [5] C. Surcouf, S. Heng, C. Pierre-Audigier, V. Cadet-Daniel, A. Namouchi, A. Murray, B. Gicquel, B. Guillard. **Molecular detection of fluoroquinolone-resistance in multi-drug resistant tuberculosis in Cambodia suggests low association with XDR phenotypes**. BMC Infect. Dis., 2011, 11, 25528.
- [6] Zanfardino A.; Pizzo, E.; Di Maro, A.; Varcamonti, M.; D'Alessio, G. **The bactericidal action on *Escherichia coli* of ZF-RNase-3 is triggered by the suicidal action of the bacterium OmpT protease**. 2010. FEBS Journal 277:1921- 28.
- [7] Ibrahim HR, Inazaki D, Abdou A, Aoki T, Kim M. **Processing of lysozyme at distinct loops by pepsin: a novel action for generating multiple antimicrobial peptide motifs in the newborn stomach**. 2005. Biochim Biophys Acta 1726(1):102:14.
- [8] Gifford JL, Hunter HN, Vogel HJ. **Lactoferricin: a lactoferrin-derived peptide with antimicrobial, antiviral, antitumor and immunological properties**. Cell Mol Life Sci.23 2005;62(22):2588-98.
- [9] Sinha M, Kaushik S, Kaur P, Sharma S, Singh TP. **Antimicrobial lactoferrin peptides: the hidden players in the protective function of a multifunctional protein**. Int J Pept. 2013;2013:390230.
- [10] Papareddy P, Rydengård V, Pasupuleti M, Walse B, Mörgelin M, Chalupka A, Malmsten M, Schmidtchen A. **Proteolysis of human thrombin generates novel host defense peptides**. PLoS Pathog. 2010;6(4):e1000857.
- [11] Kasetty G, Papareddy P, Kalle M, Rydengard V, Morgelin M, Albiger B, et al. **Structure activity studies and therapeutic potential of host defense peptides of human thrombin**. Antimicrob Agents Chemother. 2011;55(6):2880-90. 363- 74.
- [12] Lai Y, Gallo RL. **AMPed up immunity:how antimicrobial peptides have multiple roles in immune defense**, 2009. Mar;30(3):131-41.
- [13] Wu WK, Wong CC, Li ZJ, Zhang L, Ren SX, Cho CH. **Cathelicidins in inflammation and tissue repair: Potential therapeutic applications for**

gastrointestinal disorders, 2010. Acta Pharmacol Sin. Sep;31(9):1118-22.

[14] Brown K., Hancock REW. **Cationic host defense (antimicrobial) peptides**, 2006. Current Opinion in Immunology 18:24-30-94.

[15] Ramos R, Silva JP, Rodrigues AC, Costa R, Guardão L, Schmitt F, Soares R, Vilanova M, Domingues L, Gama M. **Wound healing activity of the human antimicrobial peptide LL37**, 2011. Peptides. Jul;32(7):1469-76.

[16] Papareddy P, Rydengård V, Pasupuleti M, Walse B, Mörgelin M, Chalupka A, Malmsten M, Schmidtchen A. **Proteolysis of human thrombin generates novel host defense peptides**. PLoS Pathog. 2010;6(4):e1000857.

[17] Koczulla R, von Degenfeld G, Kupatt C, Krötz F, Zahler S, Gloe T, Issbrücker K, Unterberger P, Zaiou M, Lebherz C, Karl A, Raake P, Pfosser A, Boekstegers P, Welsch U, Hiemstra PS, Vogelmeier C, Gallo RL, Clauss M, Bals R. **An angiogenic role for the human peptide antibiotic LL-37/hCAP-18**. J Clin Invest. 2003;111(11):1665-72.

[18] Salvado MD, Di Gennaro A, Lindbom L, Agerberth B, Haeggström JZ. **Cathelicidin LL-37 induces angiogenesis via PGE2-EP3 signaling in endothelial cells, in vivo inhibition by aspirin**. Arterioscler Thromb Vasc Biol. 2013 Aug;33(8):1965-72.

[19] Kim A. Brogden, Mark Ackermann, Paul B. McCray, Jr., Brian F. Tack. **Antimicrobial peptides in animals and their role in host defenses**. International Journal of Antimicrobial Agents 22 (2003) 465/478.

[20] Nakatsuji T1, Gallo RL. **Antimicrobial peptides: old molecules with new ideas**. J Invest Dermatol. 2012 Mar;132(3 Pt 2):887-95.

[21] Delves-Broughton J, Blackburn P, Evans RJ, Hugenholtz J. **Applications of the bacteriocin, nisin**. Antonie Van Leeuwenhoek. 1996;69(2):193-202.

[22] Lönnerdal B. **Infant formula and infant nutrition: bioactive proteins of human milk and implications for composition of infant formulas**. Am J Clin Nutr. 2014 Mar;99(3):712S-7S.

[23] J W. Lillard, Jr., P N. Boyaka, O Chertov, J J. Oppenheim, J R. McGhee. **Mechanisms for induction of acquired host immunity by neutrophil peptide defensins** Proc Natl Acad Sci U S A. 1999; 96(2): 651–656.

[24] Easton DM1, Nijnik A, Mayer ML, Hancock RE. **Potential of immunomodulatory host defense peptides as novel anti-infectives**. Trends Biotechnol. 2009 ;27(10):582-90.

[25] Chandrudu S, Simerska P, Toth I. **Chemical methods for peptide and protein production**. Molecules. 2013 Apr 12;18(4):4373-88.

[26] Li Y. **Carrier proteins for fusion expression of antimicrobial peptides**

in *Escherichia coli*. Biotechnol Appl Biochem. 2009 Jul 6;54(1):1-9.

[27] Li Y. **Recombinant production of antimicrobial peptides in Escherichia coli: a review.** 2011 Protein Expr Purif 80: 260-267.

[28] Peng Li, Xiang Li, Rathi Saravanan, Chang Ming Li and Susanna Su Jan Leong. **Antimicrobial macromolecules: synthesis methods and future applications.** 2012. RSC Adv.,2, 4031-4044

[29] Zhou QF, Luo XG, Ye L, Xi T. **High-level production of a novel antimicrobial peptide perinerin in Escherichia coli by fusion expression.** (2007) Curr Microbiol 54: 366-370.

[30] Moon JY, Henzler-Wildman KA, Ramamoorthy A. **Expression and purification of a recombinant LL-37 from Escherichia coli.** (2006) BiochimBiophys Acta 1758: 1351-1358.

[31] Beaulieu L, Tolkatchev D, Jette JF, Groleau D, Subirade M. **Production of active pediocin PA-1 in Escherichia coli using a thioredoxin gene fusion expression approach: cloning, expression, purification, and characterization.** (2007) Can J Microbiol 53: 1246-1258.

[32] Wu G, Deng X, Li X, Wang X, Wang S, et al. **Application of immobilized thrombin for production of S-thanatin expressed in Escherichia coli.** (2011) Appl Microbiol Biotechnol 92: 85-93.

[33] Feng XJ, Wang JH, Shan AS, Teng D, Yang YL, et al. **Fusion expression of bovine lactoferricin in Escherichia coli.** (2006). Protein Expr Purif 47: 110- 117.

[34] Crimmins DL, Mische SM, Denslow ND. **Chemical cleavage of proteins in solution.** (2005). Curr Protoc Protein Sci Chapter 11: Unit 11 14.

[35] Pane K, Durante L, Pizzo E, Varcamonti M, Zanfardino A, Sgambati V, Di Maro A, Carpentieri A, Izzo V, Di Donato A, Cafaro V, Notomista E. **Rational design of a carrier protein for the production of recombinant toxic peptides in Escherichia coli,** 2016. PLOS one 11(1):e0146552. Epub 2016/01/25.

[36] Notomista E, Cafaro V, Fusiello R, Bracale A, D'Alessio G, Di Donato A. **Effective expression and purification of recombinant onconase, an antitumor protein.** FEBS Lett. 1999; 463(3):211–5. Epub 1999/12/22.

[37] Notomista E, Catanzano F, Graziano G, Dal Piaz F, Barone G, D'Alessio G, et al. **Onconase: an unusually stable protein.** Biochemistry. 2000; 39(30):8711–8. Epub 2000/07/29.

[38] Bornstein P, Balian G. **Cleavage at Asn-Gly bonds with hydroxylamine.** Methods Enzymol. 1977; 47:132–45. Epub 1977/01/01.

[39] Dobson CB1, Sales SD, Hoggard P, Wozniak MA, Crutcher KA. **The receptor-**

binding region of human apolipoprotein E has direct anti-infective activity. J Infect Dis. 2006 Feb 1;193(3):442-50. Epub 2005 Dec 28.

[40] Kelly BA, Harrison I, McKnight A, Dobson CB. **Anti-infective activity of apolipoprotein domain derived peptides in vitro: identification of novel antimicrobial peptides related to apolipoprotein B with anti-HIV activity.** BMC Immunol. 2010 Mar 18;11:13. doi: 10.1186/1471-2172-11-13.

[41] Lee J. H, Minn I, Park CB, Kim SC. **Acidic peptide-mediated expression of the antimicrobial peptide buforin II as tandem repeats in Escherichia coli.** 1998. Protein Expression and Purification. Feb;12(1):53–60 (1998).

[42] Terry AS, Poulter L, Williams DH, Nutkins JC, Giovannini MG, Gibson BW. **The cDNA sequence coding for prepro-PGS (prepro-magainins) and aspects of the processing of this prepro-polypeptide.** The Journal of Biological Chemistry 1988 Apr 25;263(12):5745-51.

[43] Green MR, Hughes H, Sambrook J, MacCallum P, editors. **Molecular Cloning: A Laboratory Manual.** 4th ed: Cold Spring Harbor laboratory Press; 2012.

[44] Laemmli UK. **Cleavage of structural proteins during the assembly of the head of bacteriophage T4.** Nature. 1970; 227(5259):680–5.

[45] Steck G, Leuthard P, Burk RR. **Detection of basic proteins and low molecular weight peptides in polyacrylamide gels by formaldehyde fixation.** Anal Biochem. 1980; 107(1):21–4. Epub 1980/09/01.

[46] Zanfardino A.; Pizzo, E.; Di Maro, A.; Varcamonti, M.; D'Alessio, G. **The bactericidal action on Escherichia coli of ZF-RNase-3 is triggered by the suicidal action of the bacterium OmpT protease.** 2010. FEBS Journal 277:1921- 28.

[47] Wiegand I, Hilpert K, Hancock RE. **Agar and broth dilution methods to determine the minimal inhibitory concentration (MIC) of antimicrobial substances.** Nat Protoc. 2008;3(2):163-75.

[48] Tamburino R, Severino V, Sandomenico A, Ruvo M, Parente A, Chambery A, Di Maro A. **De novo sequencing and characterization of a novel Bowman-Birk inhibitor from Lathyrus sativus L. seeds by electrospray mass spectrometry.** Molecular BioSystems 2012, 8, 3232–3241.

[49] Pane K, Durante L, Crescenzi O, Cafaro V, Pizzo E, Varcamonti M, Zanfardino A, Izzo V, Di Donato A, Notomista E. **Antimicrobial potency of cationic antimicrobial peptides can be predicted from their amino acid composition: application to the detection of “cryptic” antimicrobial peptides.** 2017. Journal of Theoretical Biology-D-16-00555.

[50] Kageyama T, Ichinose M, Miki K, Tanji M, Takanashi K. **Difference of activation process and structure of activation peptides in human pepsinogen**

A and Progastricsin. J. Biochem. 1989:105, 15-22.

[51] Rydengård V, Olsson AK, Mörgelin M, Schmidtchen A. **Histidine-rich glycoprotein exerts antibacterial activity.** FEBS J. 2007 Jan;274(2):377-89.

[52] Kaiser D. **A microbial genetic journey.** 2006. Annu Rev Microbiol 60:1-25.

[53] Kaiser D. **Coupling cell movement to multicellular development in myxobacteria.** 2003. Nat Rev Microbiol 1:45-54.

[54] Shimkets L. J. **Intercellular signaling during fruiting-body development of Myxococcus xanthus.** 1999. Annu Rev Microbiol 53:525-49.

[55] McBride M. J. **Bacterial gliding motility: multiple mechanisms for cell movement over surfaces.** 2001. Annu Rev Microbiol 55:49-75.

[56] Hodgkin J, and Kaiser D. **Cell-to-cell stimulation of movement in nonmotile mutants of Myxococcus.** 1977. Proc Natl Acad Sci U S A 74:2938-2942.

[57] Arnold JW, and Shimkets LJ. **Inhibition of cell-cell interactions in Myxococcus xanthus by congo red.** 1988. J Bacteriol 170:5765-70.

[58] Bowden MG, and Kaplan HB. **The Myxococcus xanthus lipopolysaccharide O-antigen is required for social motility and multicellular development.** 1998. Mol Microbiol 30:275-84.

[59] Li Y, Sun H, Ma X, Lu A, Lux R, Zusman D and Shi W. **Extracellular polysaccharides mediate pilus retraction during social motility of Myxococcus xanthus.** 2003. Proc Natl Acad Sci U S A 100:5443-8.

[60] Wall D, Kaiser D. **Type IV pili and cell motility.** 1999. Mol Microbiol 32:1-10.

[61] Wolgemuth C, Hoiczky E, Kaiser D and Oster G. **How myxobacteria glide.** 2002. Curr Biol 12:369-77.

[62] Mignot,T, Shaevitz JW, Hartzell PL, and Zusman DR. **Evidence that focal adhesion complexes power bacterial gliding motility.** 2007. Science 315:853-6.

[63] O'Connor K.A, Zusman DR. **Behavior of peripheral rods and their role in the life cycle of Myxococcus xanthus.** 1991. J Bacteriol 173:3342-55.

[64] Zusman DR, Scott AE, Yang Z, Kirby JR, **Chemosensory pathways, motility and development in Myxococcus xanthus.** 2007. Nature Reviews/Microbiology. Nov;5(11):862-72.

[65] Berleman JE, Scott J, Chumley T, Kirby JR. **Predataxis behavior in Myxococcus xanthus.** 2008. Proc Natl Acad Sci USA. Nov 4;105(44):17127-32. doi: 10.1073/pnas.0804387105. Epub 2008 Oct 24.

[66] Ward MJ, Zusman DR. **Regulation of directed motility in Mixococcus**

xanthus. 1997. Mol Microbiol. 1997 Jun;24(5):885-93.

[67] Yang Z, Geng Y, Xu D, Kaplan HB, Shi W. **A new set of chemotaxis homologues is essential for Myxococcus xanthus social motility**. Mol Microbiol. 1998 Dec;30(5):1123-30.

[68] Kirby JR, Zusman DR. **Chemosensory regulation of developmental gene expression in Myxococcus xanthus**. Proc Natl Acad Sci U S A. 2003 Feb 18;100(4):2008-13. Epub 2003 Feb 3.

[69] Bustamante VH, Martínez-Flores I, Vlamakis HC, Zusman DR. **Analysis of the Frz signal transduction system of Myxococcus xanthus shows the importance of the conserved C-terminal region of the cytoplasmic chemoreceptor FrzCD in sensing signals**. Mol Microbiol. 2004 Sep;53(5):1501-13.

[70] Kaiser D, Robinson M, Kroos L. **Myxobacteria, Polarity, and Multicellular Morphogenesis**. Cold Spring Harb Perspect Biol. 2010 Aug; 2(8): a000380. doi: 10.1101/cshperspect.a000380.

[71] Yang Z, Geng Y, Xu D, Kaplan HB, Shi W. **A new set of chemotaxis homologues is essential for Myxococcus xanthus social motility**. Molecular microbiology, December 1998. DOI: 10.1046/j.1365-2958.1998.01160.x

[72] Trudeau KG, Ward MJ, Zusman DR. **Identification and characterization of FrzZ, a novel response regulator necessary for swarming and fruiting-body formation in Myxococcus xanthus**. Molecular microbiology, May 1996. DOI: 10.1046/j.1365-2958.1996.5521075.x

[73] Bilwes AM, Alex LA, Crane BR, Simon MI. **Structure of CheA, a signal-transducing histidine kinase**. Cell. 1999 Jan 8;96(1):131-41.

[74] Reebye V, Frillinga A, Hajitoub A, Nicholls JP, Habiba NA, Mintza PJ. **A perspective on non-catalytic Src homology (SH) adaptor signalling proteins**. Cellular Signalling. Volume 24, Issue 2, February 2012, Pages 388–392.

[75] McBride MJ, Weinberg RA, Zusman DR. **“Frizzy” aggregation genes of the gliding bacterium Myxococcus xanthus show sequence similarities to the chemotaxis genes of enteric bacteria**. Biochemistry. Vol. 86, pp. 424-428, January 1989

[76] Kashefi K, Hartzell PL. **Genetic suppression and phenotypic masking of a Myxococcus xanthus frzF- defect**. Mol Microbiol. 1995 Feb;15(3):483-94.

[77] Guzzo M, Agrebi R, Espinosa L, Baronian G, Molle V, Mauriello EMF, Brochier-Armanet C, Mignot T. **Evolution and Design Governing Signal Precision and Amplification in a Bacterial Chemosensory Pathway**. Plos Genetics August 20, 2015.

[78] Li X, Fleetwood AD, Bayas C, Bilwes AM, Ortega DR, Falke JJ, Zhulin IB, Crane BR. **The 3.2 Å resolution structure of a Receptor:CheA:CheW signaling**

complex defines overlapping binding sites and key residue interactions within bacterial chemosensory arrays. *Biochemistry*. 2013 Jun 4; 52(22): 3852–3865.

[79] Moine A, Espinosa L, Martineau E, Byrne D, Notomista E, Molle V, Mignot T and Mauriello EMF. **The nucleoid as a scaffold for the assembly of bacterial signaling complexes** [SUBMITTED]

[80] Moine A, Agrebi R , Espinosa L , Kirby JR, Zusman DR, Mignot T, Mauriello EMF. **Functional Organization of a Multimodular Bacterial Chemosensory Apparatus.** *Plos Genetics*. March 6, 2014.

Appendices

List of communications

1. M. Verrillo, K. Pane, E. Pizzo, M. Varcamonti, A. Zanfardino, M. Siepi, **A. Avitabile**, A. Di Donato, E. Notomista, V. Cafaro. “*Efficient production and labeling of recombinant peptides endowed with a N-terminal cysteine residue*”. Bologna, March 30th-April 1th 2016.
2. K. Pane, V. Cafaro, **A. Avitabile**, A. Bosso, E. Pizzo, E. Notomista, A. Di Donato “*A novel carrier protein for AMPs production*” 5th Antimicrobial International Meeting on Antimicrobial Peptides, Burlington House 7th-8th September 2015.
3. **A. Avitabile**, V. Cafaro, K. Pane, A. Bosso, E. Pizzo, E. Notomista, A. Di Donato. “*The activation peptide of human pepsinogen is an antimicrobial peptide*”. 5th Antimicrobial International Meeting on Antimicrobial Peptides, Burlington House 7th-8th September 2015.
4. A. Bosso, V. Sgambati, K. Pane, **A. Avitabile**, A. Di Maro, E. Pizzo. “*A novel source of microbial agents: characterization of an antimicrobial peptide from PD-L4, a type 1 ribosome inactivating protein from Phytolaccadioica L.*” 5th Antimicrobial International Meeting on Antimicrobial Peptides, Burlington House 7th-8th September 2015.
5. A. Bosso, K. Pane, **A. Avitabile**, M. Verrillo, A. Del Gatto, L. Zaccaro, L. Pirone, S. Di Gaetano, R. Fattorusso, D. Diana, E. Pedone, V. Cafaro, E. J. A. Veldhuizen, E. Notomista, E. Pizzo. “*Cryptic anti-microbial peptides in human secretory proteins: the case of H11 β (235-261)*”. 15th Naples Workshop on Bioactive Peptides. June 23rd-25th 2016.

Experience in foreign laboratories

Stage at “Centre National de la Recherche Scientifique (CNRS)” for the identification of regulation check points in a *Myxococcus xanthus* chemosensory system, “Laboratoire de Chimie Bactérienne (LCB)”, University of Marseille, Marseille, France (2^{sd} May 2016- 29th July 2016). The work was supervised by Dr. Tam Mignot, the director of the Mignot team and Emilia Mauriello researcher of the Mignot team.

Research activity in scientific Institutions abroad



From May 2^o to July 29^o, 2016, the research activity of Dr. Avitabile has been carried out at the Centre National de la Recherche Scientifique, Marseille (France), in the laboratory of the "Chimie Bactérienne". The work was supervised by Dr. Mignot and Dr. Mauriello.





Dr. Târn Mignot
Laboratoire de Chimie Bactérienne, UMR7283
CNRS
31 Chemin Joseph Aiguier
13402 Marseilles, France

Prof. Giovanni Sanna, Director
PhD School in Biotechnological Sciences
Dept. Organic Chemistry and Biochemistry
Monte S. Angelo
Via Cynthia, 4 – 80126 Naples, Italy
Fax 0039081674313
sanna@unina.it

Marseilles 30-06-2016

This is to certify that Angela Avitabile, student of the PhD course in Biotechnological Sciences -29°cycle-, attended seminars and research activities for her thesis in my research group at the Laboratoire de Chimie Bactérienne, CNRS (Marseille, France) from May 2nd 2016 to July 29th.

Sincerely,

Târn Mignot

ACKNOWLEDGMENTS

I wish to express my gratitude to Dr. Tam Mignot and Emilia Mauriello for giving me the opportunity to work in their laboratories.

Moreover, I would like to thank Annick, Valerie, Laetitia, Julie, Seb, Israel, Audrey, Roman, Salim and Laura for their help and friendship during my period abroad.